MANIPULATION AND SORTING OF CELL-LADEN HYDROGEL MICROCAPSULES WITHIN MICROFLUIDIC ENVIRONMENT

KARAN DHINGRA

Thesis is submitted to the Faculty of Engineering in partial fulfillment of requirements for the degree of

Master of Applied Science

in

Biomedical Engineering

Ottawa Carleton Institute for Biomedical Engineering
University of Ottawa
Ottawa, Ontario

ABSTRACT

Encapsulating cells within semi-permeable hydrogel material has been shown to boost the therapeutic effectiveness of stem cell therapy in certain applications. Cell encapsulation promotes high retention and engraftment rates, and protects against attack from the immune system of the host, as these are challenges often seen in utilizing stem cells in suspension alone. Leveraging droplet-based microfluidics has yielded a platform capable of producing monodispersed microcapsules embedded with cells at high throughput, typically achieved by mixing an aqueous hydrogel solution that contains cells with an immiscible liquid (oil) in a flow focusing geometry. However, encapsulation using microfluidics results in randomized generation of empty and cell-laden microcapsules, following Poisson statistics, raising the need to institute a successful sorting mechanism, thereby increasing occupancy and ultimately purifying the desired sample. In this thesis we propose a sorting strategy by combining two conceptual mechanisms of electrophoresis (EP) and deterministic lateral displacement (DLD). Different varieties of microcapsules were characterized for EP and DLD respectively. Leveraging these differences was used in a device combining both of the concepts towards sorting of empty and cell-laden microcapsules.

STATEMENT OF ORIGINALITY

The content presented in this thesis is the product of original work performed by Karan Dhingra at the University of Ottawa under the supervision of Professor Michel Godin. All the assistance received in preparing this thesis and their respective sources have been acknowledged.

In partial fulfillment of the requirements for the degree of Master of Science (Biomedical Engineering) at the University of Ottawa, this work was presented at the Ottawa Carleton Institute for Biomedical Engineering Seminar Series: Karan Dhingra and Michel Godin, Manipulation and Sorting of Cell-laden Hydrogel Microcapsules within Microfluidic Environment, Ottawa Carleton Institute for Biomedical Engineering, April, 2019. A poster on the same topic was also presented at the Solutions for Cardio-pulmonary Organ Repair and Regeneration (SCORR) Scientific Research Day: Karan Dhingra and Michel Godin, Manipulation and Sorting of Cell-laden Hydrogel Microcapsules within Microfluidic Environment, March 2019.

STATEMENT OF CONTRIBUTION

The entirety of this document was written by the author. All figures and tables were created by the author unless otherwise mentioned in the caption. The work presented was largely performed by the author including, photomask designs, fabrication of devices (photolithography, PDMS mold replication), testing of devices, and electrical setup for EP and DLD- EP experiments, encapsulation of cells and data analysis. The cell encapsulation setup along with the LabVIEW® code for the control of pressure regulators and heating/cooling block was created by Professor Michel Godin. The cell encapsulation device in the same figure was designed primarily by Nicolas Monette-Catafard with added modifications by Dr. Ainara Benavente-Babace.

ACKNOWLEDGEMENTS

Throughout my graduation journey, Dr. Michel Godin has been supportive and encouraging at every step of the way. His expertise and motivation was invaluable in providing the support that I needed to complete this research study. His regular feedback provided the stepping stone I needed to improve my overall skill-set as a researcher. My gratitude goes out to Adefemi Habib Adeyemi for helping me build a strong foundation for the conceptual knowledge pertaining to cell encapsulation, cell culturing, and fabrication of microfluidic devices. I would also like to thank Dr. Ali Najafi Sohi for his valuable input in providing alternative solutions for troubleshooting experimental protocols. In addition to this, I would like to express my gratitude to past and present members of the Godin Lab for productive discussions: Dr. Ainara Benavente, Eric Beamish, Nicholas Soucy, Kaitlyn Kean, Rushi Panchal and Enas Azhari. Furthermore, I would like to thank members of the Pelling Lab for giving me access to their cell culture room.

Special thanks to my parents Sunita and Vijay Dhingra and my sister Neha Saurabh Dhingra for their constant support through my Master's journey. Thank you to Saloni Verma, for all her love and support.

LIST OF FIGURES

LIST OF TABLES

TABLE OF CONTENTS

CHAPTER 1

INTRODUCTION

1.1 Background

Undifferentiated cells, otherwise known as stem cells, are extensively being used in applications for regenerative medicine and disease therapeutics, due to the ease with which these cells can be directed to develop into different cell types in the human body. Stem cells may be obtained from the same person (autologous) or from a donor (allogenic). Since allogenic stem cells are of foreign nature to the patient, there are more immunogenic risks associated with them. With these types of cells, a delivery method is required in order to administer the cells into the patient, i.e., cell mediated therapy. In order to safely deliver cells into a patient, they are generally immobilized within a biocompatible material such as hydrogel to help suppress the immune effects. In addition, the hydrogels and scaffolds offer mechanical support to the infarcted tissue. The biggest hurdle in most cell-based therapy is low engraftment [1] and persistent rates once the cells are introduced into the target tissue. Cell encapsulation is a promising way to mitigate all three of these issues.

Manipulating and controlling fluids at small scales, well known as microfluidics, enables high-throughput production of cell-laden microcapsules. However, since the encapsulation process is dependent upon Poisson statistics, occupancies in the encapsulated cells remains inconsistent. This essentially means that the microcapsules generated may have 0, 1, 2… cells per microcapsule depending on the encapsulation conditions and initial cell concentrations. The goal of this study is to tackle this challenge, and increase this occupancy by developing a sorting method that can remove unoccupied microcapsules from the final sample. This will be done by implementing an on-chip microcapsule sorting technique, to differentiate empty microcapsules from occupied ones.

1.2 Microfluidics

Due to its microscopic nature, microfluidics offers several advantages over traditional bulk methods including reduced sample consumption rates [2], automation [3] and the prospect of lab-on-a-chip (LOC) [4] integration. The behavior of fluids across a microfluidic channel is governed by various flow-regimes and can be broadly categorized into, laminar and turbulent flow.

The laminar flow regime follows a smooth pattern, in an orderly manner (infinitesimal parallel layers), thus remaining stable throughout the microfluidic channel. Turbulent flow on the other hand follows a structure of inherent instability [5]. Both flow regimes are shown in *Figure 1*.

Both flow patterns are characterized by the Reynolds number, which was first discovered by Osborne Reynolds and is the ratio between inertial forces and viscous forces,

$$Re = \frac{\rho V L}{\mu} = \frac{Inertial\ Forces}{Viscous\ Forces} \qquad (1)$$

ρ = density of the fluid (Kg/m^3),

V = velocity of the fluid (m/s),

μ = viscosity of fluid (Ns/m^2),

L = length or diameter of the fluid (m),

Because microfluidic channel lengths are extremely small, the length (L) dominates the equation generally resulting in a low Reynolds number (<<1), which in turn correlates broadly to the laminar flow [6]. For microfluidic devices ranging from 1-100 μm radius/height , general considerations when using water as a fluidic medium are, viscosity: $8.90*10^{-4}$ Pa at 25°C, density: 1 g/mL, with an average flow velocity: 1 μm/s – 1 cm/s.

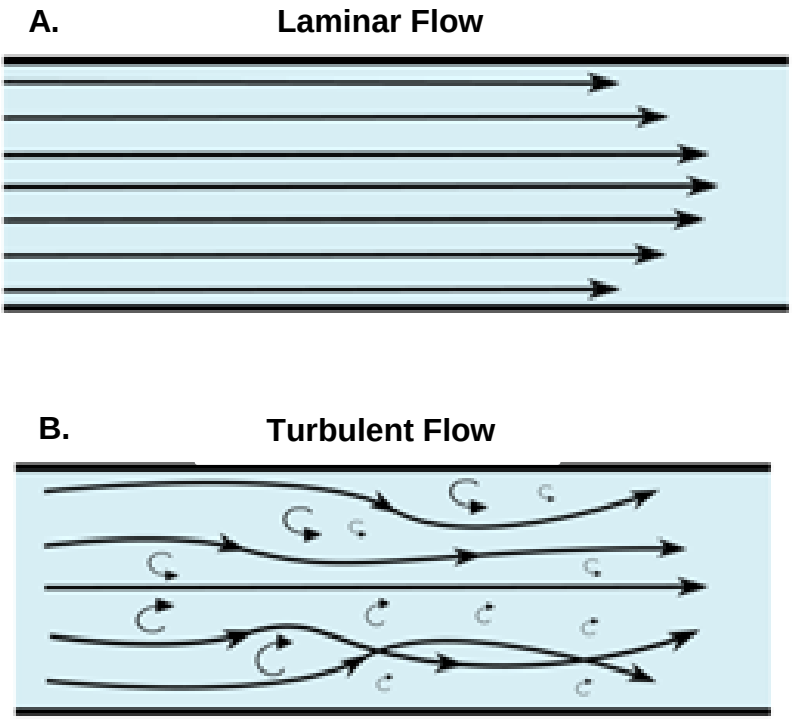

Figure 1 A. Illustration of laminar flow vs. turbulent flow, where the arrow lines represent flow streamline pathways of particles in motion inside a microfluidic channel. Laminar flow is characterized by infinitesimal parallel flow lines resulting in little to no mixing, as seen in microfluidics [7]. B. On the other hand, turbulent flow is characterized by chaotic behavior due to changes in pressure and flow velocity, and is not a common occurrence in microfluidics. [Figure adopted from CFD support]

1.3 Droplet Based Microfluidics

1.3.1 Theory and Applications

"Droplet microfluidics" aims to generate uniform and size controlled volumes of fluids in immiscible phases with a low Reynolds number, all within laminar flow regimes. The ability to encapsulate biological samples (e.g. cells, bacteria, biomolecules, etc.) within micro-droplets of Pico liter to Nano liter volumes has been demonstrated in a variety of applications in chemical and biological sciences as well as LOC [8].

Microfluidic droplets are generated on-chip by precisely mixing two immiscible fluids. Typically, these fluids are introduced using pressure-driven flow. For aqueous micro-capsules,

they are formed and carried down a microchannel by an oil-based carrier fluid. These microcapsules are often seen as individual micro-reactors, where reagent mixing can be accelerated due to the small reaction volumes [9].

1.3.2 Droplet Formation

Droplet formation can be explained by understanding the dimensionless quantity of Capillary number (C_a), which demonstrates a relationship between viscous forces and capillary forces occurring between two immiscible liquids [10]. The Capillary number is governed by the equation,

$$C_a = \frac{\mu V}{\gamma} \qquad (2)$$

Where,

μ = viscosity of continuous phase (oil) (Ns/m^2)

V = flow velocity of continuous phase (m/s)

γ = interfacial tension between the continuous and dispersed (hydrogel) phase (N/m)

When the Capillary number is low, the interfacial tension forces dominate viscous forces and flow results in droplet breakup. On the contrary, when the capillary number is high, surface forces are dominated by viscous forces, resulting long liquid plugs being formed instead of droplets [11]. Microfluidic methods for droplet formation may be divided into [12],

- **Active:** utilizes external force and energy to create droplets, for example, in cases of highly viscous solutions
- **Passive:** mixing of two immiscible liquids, i.e., a dispersed phase into a continuous phase

In this study passive methods are adopted for micro-droplet formation. The droplet formation can occur via flow focusing device geometry. The technique consists of three channels, where the dispersed phase (aqueous) is squeezed by two orthogonally flowing continuous phases (oil) [13] as shown in *Figure 2*.

The number and size of droplets produced depend on parameters such as the flow rates, channel dimensions and capillary number [14]. By controlling the flow rates, the size of droplets

produced can be decreased or increased. Changing the dimensions of aperture also has an effect on the size of droplets produced; bigger aperture allow larger droplets to be produced [15].

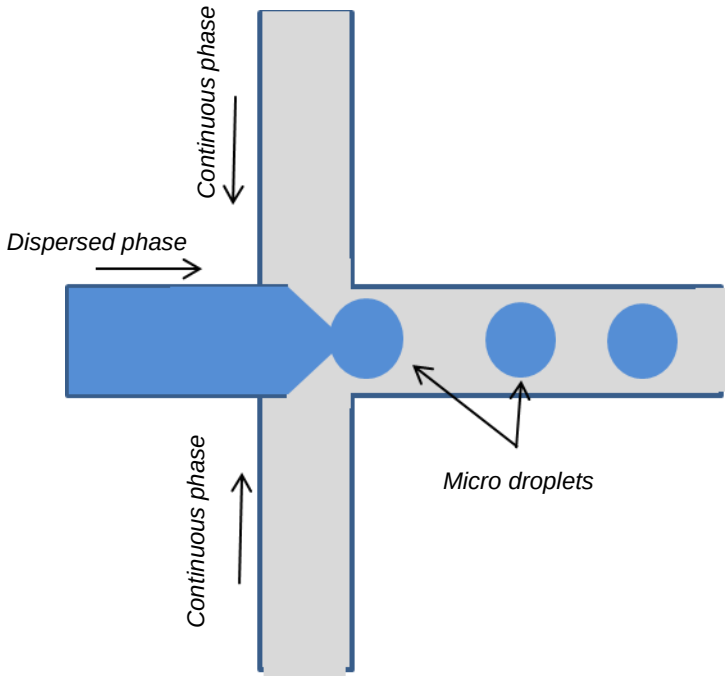

Figure 2. Droplet-based microfluidics demonstrating flow focusing geometry (average channel width ~300µm and height ~100 µm where, spherical micro-droplets are generated due to surface energy distribution from two continuous phases from a dispersed phase of aqueous solution.

1.4 Stem Cell Therapy

Stem cells are unspecialized cells that have the ability to self-renew and generate multiple cell types. They have shown therapeutic ability to treat regenerative diseases [16]. Cell-therapy aims at applying these undifferentiated cells to a target location where they can develop into any specialized cell type.

Stem cells, either autologous or allogeneic, have their respective advantages and disadvantages. Regardless of the type, certain limitations exist, which need to be addressed. One such limitation is cell retention, as it helps in understanding the cell's ability to remain intact at the site of implant, which is essential for an improved therapeutic outcome (some studies have shown less than 10% retention rate over a 24 hour period) [17]. One measure taken to overcome this challenge includes increasing the total number of injected cells; however, this leads to a new

set of problems such as graft versus host disease (GVHD) [18]. Another factor which limits the therapeutic effects of stem cells inside a biological system is metabolic rate, as cells might not receive enough nutrients to survive within the host body [19]. In addition to these disadvantages, allogeneic stem cell therapy is subjected to high immune risks like graft rejections, due to the use of foreign donor cells [20].

Droplet microfluidics shows great potential to improve stem cell-based therapy by isolating (encapsulating) stem cells within a non-living semi-permeable material. Encapsulation technology provides a medium for transport of stem cells to increase the therapeutic outcome while avoiding the limitations of cell based-therapy mentioned above [21].

1.5 Cell Encapsulation

Cell encapsulation immobilizes cells within a hydrogel based material. It has been shown to provide high retention rates [22], engraftment [23] and ultimately higher cell viability [24]. Encapsulation of stem cells thus provides a medium of safe transport, also allowing bi-direction flow as depicted in *Figure 3*. It allows an inward flow of nutrients, growth factors cell-signaling molecules and oxygen, to maintain the cell metabolism while facilitating the outward flow of waste and therapeutic products.

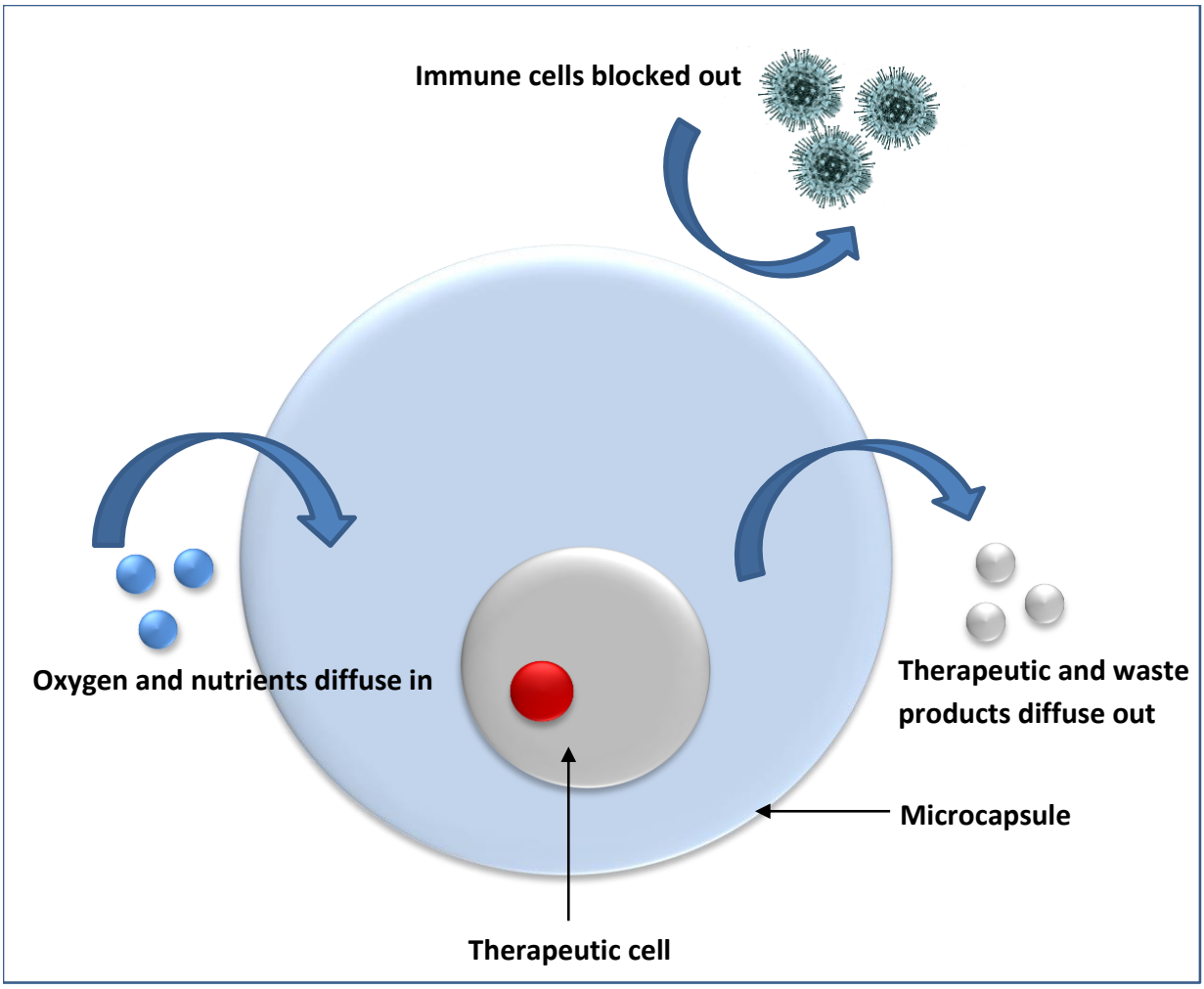

Figure 3. Schematic diagram of an encapsulated cell in a semi-permeable hydrogel microcapsule. The hydrogel capsule allows the entry of oxygen and nutrients while maintaining outward flow of therapeutic and waste products. The hydrogel layer also blocks out immune cells protecting the cell within.

1.5.1 Hydrogel

The micro droplet is composed of a hydrogel polymeric network that serves two purposes: (1) it acts as a protective shield for the stem cells against the host immune system; (2) it helps with the release of therapeutic factors. Hydrogel is a hydrophilic network of polymer chains with an ability to absorb water. Therefore, it mimics the extracellular matrix, like the one found outside cells in the host body [25]. Hydrogel is inert to normal biological processes, shows resistance to degradation, while being permeable to metabolites, is not absorbed by the body, is

biocompatible, withstands heat sterilization without damage, and can be prepared in a variety of shapes and forms [26].

These hydrogel materials include alginate and agarose [26][27]. In this work, we chose to use agarose, an FDA approved hydrogel, to generate micro droplets. Agarose is a soft hydrogel which stimulates a natural cell environment. Moreover, it is transparent which allows for easy visualization of cells under a microscope. Ultra-low gelling point agarose *(Sigma-Aldrich Type-IX, A5030)* allows the user to achieve extreme temperatures (of both hot and cold) on the microfluidic platform. At 37°C, agarose transitions from solid to liquid state, upon cooling it reverts to a gel at ~15°C. Tuning the porosity will vary the nutrient gradient across the hydrogel. The degree of porosity will have a substantial effect on mechanical properties, with the agarose stiffness increases as the porosity decreases [28].

Countertop techniques for creating hydrogel based microcapsules involve vortexing where a mixture of cells and agarose are mixed together to form microcapsules. Microcapsules created using this method show high polydispersity in their size, thereby limiting their applications in therapy, where a small monodispersed sample size is required [29]. Since the vortexing process is random in nature, there is no control over cell distribution within the micro-droplets.

Microfluidic strategy offers advantages over the vortex techniques by offering increased throughput; mono-dispersity and decreasing shear stress which tends to rupture freshly-formed micro droplets. [30] Mono-dispersity in our setup is important as it helps in providing a more potent sample to the patients as well in stem cell therapy applications where large microcapsules samples cannot be used. This is discussed in detail under *section 1.7 Cell Encapsulation technique*.

1.6 Method

1.6.1 Cell Culture

For this study, the cell model used was NIH 3T3 cells, derived from mouse embryonic fibroblasts, that are encapsulated within agarose microcapsules. These cells have a doubling rate over t=24 H. General cell culturing guidelines were followed for the process below,

The cells are kept frozen at -80 °C prior to starting a new cycle. Starting a new cycle involves thawing the frozen vial (1mL) to 37 °C, using a water bath. The vial is then transferred into a cell culture flask with 11-12 mL of fresh cell culture media (DMEM +10%FBS+1% Strep). The cell culture flask is kept inside an incubator, set at 37 °C and 5% CO_2 air atmosphere, until 80% confluency is attained i.e., until 80% of the flask surface area is covered by a cell monolayer. Before using these cells for further experimentation, they have to undergo at least one cycle of subculture post thawing.

To begin a subculture, the cell culture flask must be at 80% confluency. The primary cell culture media is aspirated and the cells are washed with 5 mL PBS (Phosphate Buffered Saline). The next step is to add 3 mL of Trypsin and incubate for 5 minutes at 37 °C and 5% CO_2 air atmosphere, this facilitates detachment of cells from the surface of the plate. Detached cells are collected inside a vial and diluted with 6 mL of fresh media. In order to count the number of cells, 10 µL of cells are collected from the 9 mL (=3 mL Trypsin + 6 mL Fresh Media) solution and added to a hemocytometer. Hemocytometer is a counting chamber device consisting of four quadrants through which one can easily count the number of cells at a given time. The remaining solution is then centrifuged and the supernatant is aspirated. Fresh media is added to the pellet and the sub-culture can continue for a specific number of cycles after seeding in a new culture plate [31].

1.6.2 Device Fabrication

Microfluidic devices are fabricated using soft lithography technique, which encompasses creation of channels embossed on a polymer attached to a glass slide. Biocompatible polymers such as Polymethylmethacrylate (PMMA), Polycarbonate (PC) and Polydimethylsiloxane (PDMS) are used to fabricate microfluidic devices, wherein, PDMS is the most commonly used polymer due to its flexibility and cost effectiveness. Previous work done in the Godin Lab outlines a microfluidic fabrication process which is capable of efficiently encapsulating cells [32].

1.6.3 Design

The microfluidic devices used in this study were designed using computer aided drawing (CAD) software, CleWIN and AutoCAD®. As seen in *Figure 4*, the cell encapsulation device comprises of three distinct sections,

- **Inlet:** The inlet allows inward flow of aqueous solution and oil through a filter to trap any impurities and contaminants
- **Micro-droplet Formation:** The second region is where cell encapsulation occurs, in which, two immiscible fluids are combined to form a micro-droplet as discussed in section *1.3.2 Droplet Formation*
- **Outlet:** The last region consists of serpentine geometrical channels to allow the droplets to cool down before reaching the outlet

A printed photomask variation used for soft-lithography is obtained via AutoCAD®blueprints from the CAD/Art Services.

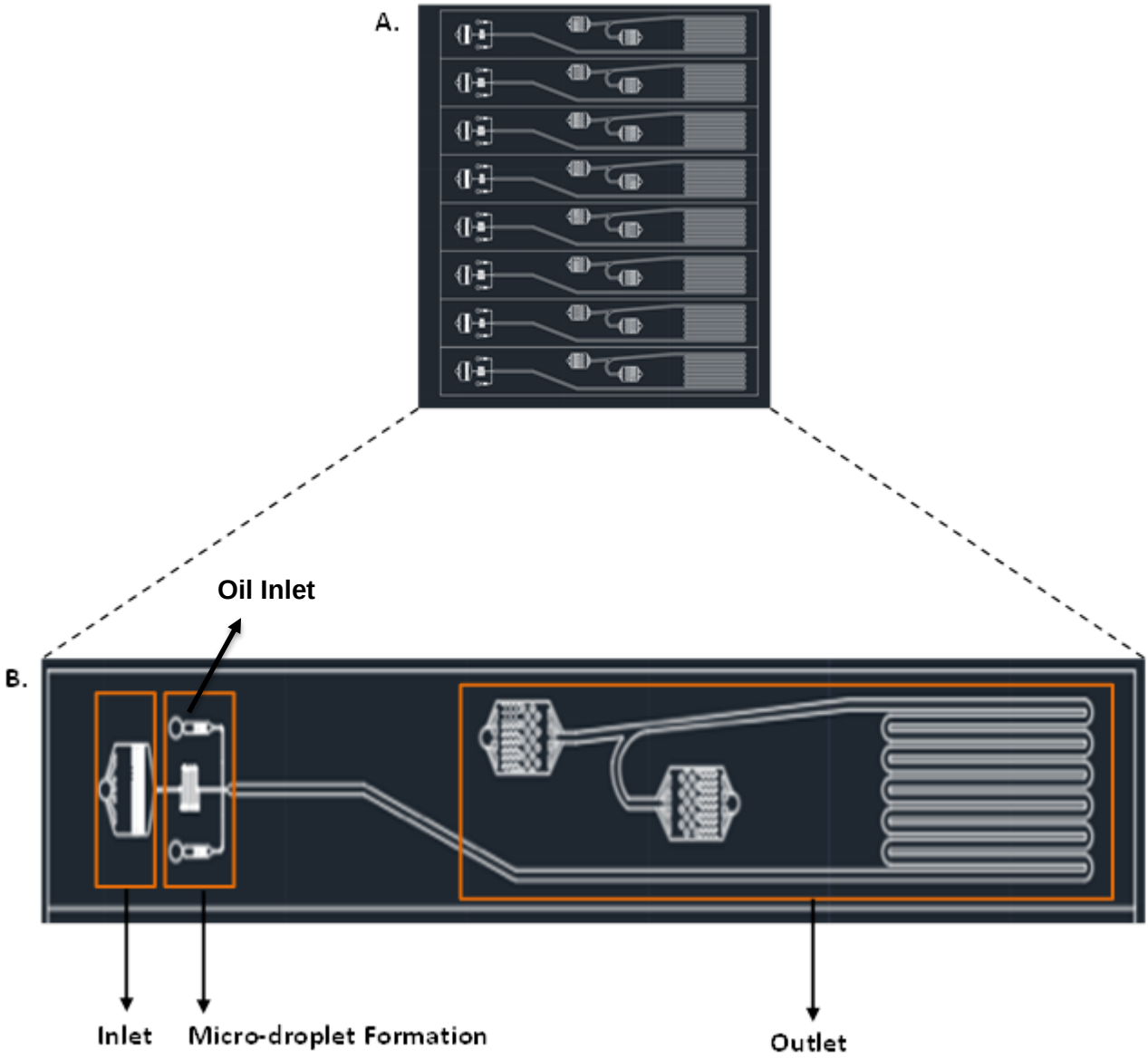

Figure 4 A. AutoCAD® drawings of multiple encapsulation devices. B. Stages of encapsulation in a single device, namely, Inlet for the entrance of agarose-cells mixture, Micro-droplet formation for the generation of microcapsules and the Outlet for the exit of the particles or sample after travelling through the microfluidic channel.

1.6.4 Soft-photolithography

Soft photolithography refers to the creation of molded patterns using photomasks, wherein, the term soft indicates the usage of a wide variety of elastomeric materials such as PDMS. The master mold is created in a clean room facility to avoid contamination and changes in temperature, humidity and pressure. These measures are taken as the master mold can be used multiple times for device fabrication. General soft-lithography guidelines were followed for the process below [33],

Cleaning and Exposure Preparation:

A new silicon wafer is first cleaned by rinsing with ethanol, acetone and isopropyl alcohol (IPA), followed by drying using N_2 air. The silicon wafer is dehydrated next using a hot plate (150 °C, 2 min). This is followed by plasma treatment of the silicon wafer (150 Watts, 5 min). Plasma treatment oxidizes the wafer, thus facilitating consistent spreading of photoresist by spin coating. In this work, we chose SU-8 photoresist for the fabrication of microfluidics features and silicon wafer mold. Since the height of photoresist achieved using a spin coater is inversely proportional to the spin speed, we used a spin speed of 1700 RPM to obtain an SU-8 film thickness of ~100 µm. Following spin coating, the silicon wafer is pre-baked at 65 °C for 5 minutes and 95 °C for 15 minutes for the SU-8 film to solidify.

Exposure:

The pre-baked SU-8 is exposed to UV light (17.6 mW/cm^2) under the photomask of the desired microfluidic design (14 seconds). This step allows features of the photomask to be imprinted on the SU-8. The exposure time is based on the desired height of the channel and the power of the UV lamp. This time can be calculated using the SU-8 2000 data sheet provided by MicoChem [33]. Following exposure, the wafer is post-baked at 65 °C for 5 minutes and 95 °C for 10 minutes.

Development:

In order to remove the excess photoresist and realize the microfluidic features, photoresist development was carried out by dipping the wafer in a flask containing SU-8

developer (1-Methoxy-2-propyl acetate) for 10 mins which is divided into 5 minutes of dipping the wafer in a flask and 5 minutes of agitating/stirring in the developer. The wafer is now rinsed with isopropyl alcohol, dried with nitrogen gun and hard-baked at 150 °C for 5 minutes.

Silanization:

Silanization prevents adhesion of PDMS to the master mold during the casting process. To achieve this, ~2 µL of the silanization agent [(Tridecaufuloro-1, 1, 2, 2- Tetrahydrooctyl) Trichlorosilane] and silicon wafer are incubated for 5 minutes inside a vacuum desiccator with the vacuum turned 'ON'. This is followed by a 24 H incubation period inside the vacuum desiccator with the vacuum turned 'OFF' [method adopted from Microfluidics/Microfabrication Facility, Harvard Medical School][34]. This forms a monolayer of Silane on the surface of the wafer or master mold. This Silane coating prevents PDMS residue from sticking to SU-8 after curing, thereby preventing damage to the master mold.

Casting:

Liquid PDMS (developed by mixing elastomer and curing agent in a 10:1 ratio [w/w]) is poured into the master mold which is then degassed for ~1 hour using a vacuum desiccator to remove air bubbles. The wafer with PDMS is then put into an oven at 70 °C for 2-3 hours for the PDMS to solidify (curing). Cured PDMS is then cut into small pieces (4x2 cm) to fit onto the glass slide. The cut PDMS pieces are punched with 0.75 mm diameter holes, to serve as inlets and outlets to microfluidic network.

Bonding:

A clean glass slide and punched PDMS sections are plasma treated at 55W for 0.8 minutes. The treatment exposes the SiO groups present on the surface of the PDMS which easily attaches to the oxidized surface of the glass slide. Post bonding, the devices are kept in the oven at 70°C for 2-3 days to achieve two goals: First, completion of PDMS to glass bonding, and secondly to turn the microfluidic channel surface chemistry into hydrophobic (which avoids wetting) and promote formation of micro-droplets [35].

1.7 Cell Encapsulation Technique

The encapsulation process for this study has been adopted by the work done in Godin Lab [36]. Experimentally; the device can produce a throughput of ~1.5 million microcapsules per hour with a precision of +/- 5% in microcapsule diameter (55-60 µm for this study). The device can take a maximum input of 10 million cells/mL before clogging. Based on the flow-focusing geometry, the device generates micro-droplets through controlled emulsification of aqueous agarose cell mixture and oil as shown in *Figure 2*.

To encapsulate cells, agarose and cells are mixed at 37°C to form a 2% agarose solution at a cell concentration of 8 million/mL. The mineral oil (containing 1.5% SPAN 80) and aqueous agarose cell mixture are sent through the corresponding micro-channels using pressure driven flow, such that the oil pinches the flow of the aqueous solution to form micro-droplets (*as shown in Figure 5*). SPAN-80 is a non-ionic surfactant that avoids coalescence between two or more microcapsules. Through thermo modules and a water circulating supply around the device setup, a temperature gradient is maintained to keep the aqueous mixture at the inlets warm and avoid pre-gelling. The droplet generation region is set to 37°C while the serpentine and the collecting outlets are set at 4°C, this is done in order to start the gelation of the agarose microcapsules. A vial containing collection media kept on ice is present at the outlet for collection of the microcapsules exiting the microfluidic device.

However, the microcapsules collected at the outlet are still in an oil phase, thus need to be filtered out. Filtering is done off-chip by a series of centrifugation processes at 2500 RPM for 3 mins, where the microcapsules settle at the bottom and oil phase (due to low density) stays on top. The oil phase is then pipetted out and the process is repeated 2-3 times. The final product is a mixture of empty and occupied microcapsules in the collection media.

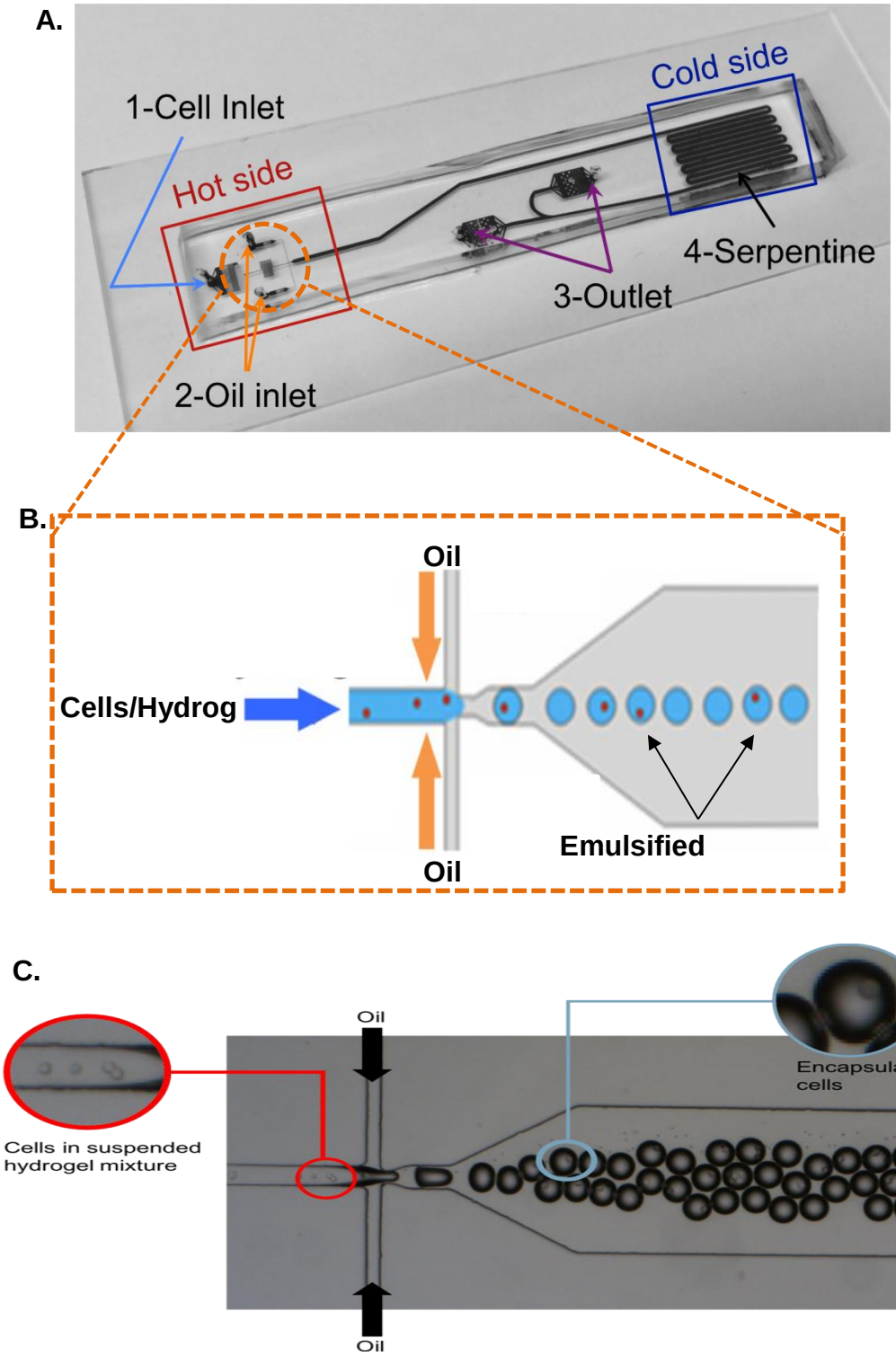

Figure 5 A. The actual microfluidic platform bonded to a glass slide. B. Schematic diagram depicting the entire encapsulation process. C. Micro-droplet formation showing the encapsulation process of 3t3 cells. [Figure 5 A. and 5 B. adopted from Dr. Ainara, Godin Lab]

1.8 Need for Sorting

As explained in section *1.5 Cell Encapsulation*, there are a wide variety of advantages of using microfluidics for creating cell-laden microcapsules. However, one problem which remains unsolved is occupancy, i.e. the possibility of having empty microcapsules (with no cells in them) as shown in *Figure 6 b*. This problem remains unresolved due to the fact that the number of cells that can be encapsulated using the droplet-based theory follows the naturally-occurring Poisson distribution [37].

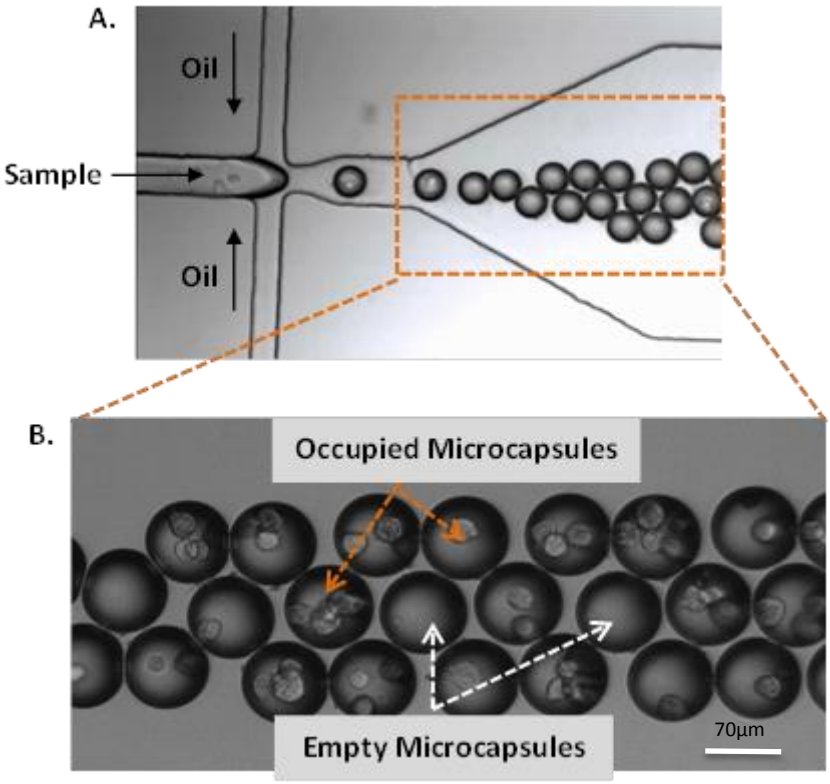

Figure6 A. Micro-droplet formation demonstrating empty microcapsules produced during encapsulation. The concentration of the cell sample is 8 million/mL and the microcapsule diameter is 50-60 µm. B. Zoomed in image of micro-capsules generated demonstrating random arrangement of cells in microcapsules. [Figure 6 B. adopted from Dr. Ainara, Godin Lab]

Poisson distribution expresses the probability of a given number of events occurring in a fixed interval of time or space, given that these events occur with a known constant rate and independently of the time since the last event. Therefore, Poisson distribution is responsible for calculating the efficiency/occupancy of encapsulation process. The probability of a microcapsule volume [V], to contain [n] cells with an initial cell concentration [d], can be expressed as (equation adapted from work done previously in the lab),

$$P(X = n, \lambda) = \frac{\lambda^n e^{-\lambda}}{n!} \quad (3)$$

With $\lambda = V \text{ x } d$

The probability of obtaining empty microcapsules increases with a decrease in microcapsule size. For example, microcapsules sized at 50 µm would have a 60% probability of generating empty microcapsules as shown in *Figure 7*. This essentially means that majority of microcapsules introduced in a patient during stem cell therapy may end up being empty, thus of no therapeutic value! Therefore, there is an essential need to sort cell-laden microcapsules, differentiating them from the empty ones, which will ultimately increase the occupancy and throughput.

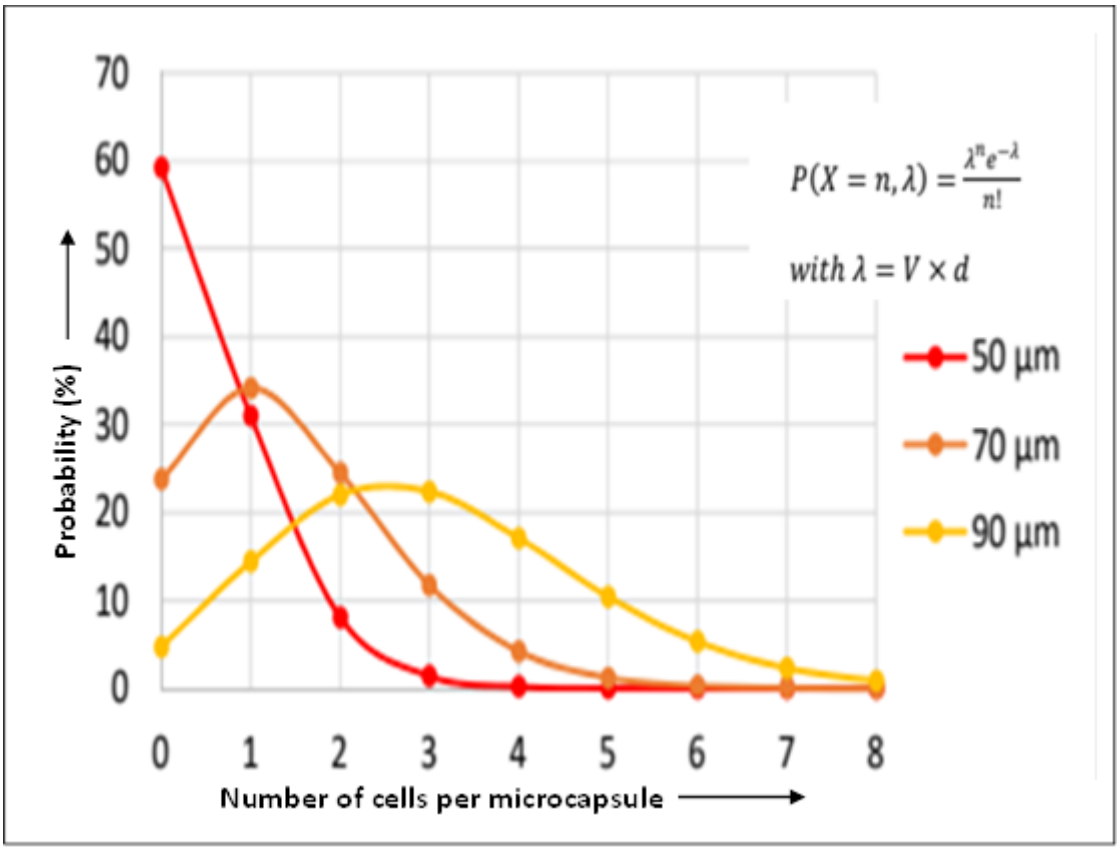

Figure 7. Trends for number of cells per microcapsule vs the probability (%) for three different microcapsule sizes [Graph made by Dr. Ainara Benavente].

In order to sort empty and occupied microcapsules, attributing factors of sorting need to be explored. The first strategy for our encapsulation setup, would be to increase the concentration of cells in the aqueous solution. It should be noted that, there is an upper limit of 10 million cells/mL, as high concentration can clog the microfluidic device, hindering efficient encapsulation. Some known factors used for sorting are,

- Size difference
- Difference in net charge

} Particle induced

1.8.1 Sorting Methods

Several sorting methods have been adopted in the past in order to isolate and separate cell-laden microcapsules. These methods tend to differentiate based on electro kinetics, magnetophoretic, optical or hydrodynamics properties of cell-laden versus empty microcapsules. These methods can broadly be divided into two groups,

- **Active**: rely on external force fields (could have a negative impact on cell biology/chemistry)
- **Passive**: rely on the inherent properties of microcapsule

A previous research study sorted empty microcapsules from pancreatic islet-laden microcapsules using the active approach, wherein, these microcapsules were made to pass through a laser-detection region, which was capable of detecting fluorescent activated cells inside the microcapsules. Upon detection of empty capsules, a non-uniform AC electric field was induced, resulting in the deflection of the microcapsules with cells to a different trajectory motion [38].

Another research group used the active approach to sort microcapsules based on their size and density, by generating standing surface acoustic waves (SSAWs) using an interdigitated transducer (IDT)[39]. With the help of SSAWs, a mixture of alginate beads (containing no cells, low number of cells or high number of cells) was separated into three distinct flow pathways, which were then collected separately through three outlets.

An interesting example of the passive sorting approach used in a research study involves using deterministic lateral displacement (DLD) to sort microcapsules based on their size [40]. A microfluidic platform was used to combine a jetting droplet generator and DLD, to encapsulate and sort individual cancer cells. The hypothesis was that any droplet which contains a cell, will be larger in size, compared to a droplet with no cell. This sample was then flown across a DLD system consisting of an array of micro-posts, which allowed smaller droplets to pass through and deflected the larger droplets in a separate pathway. Passive techniques present an advantage

over active methods by limiting the amount of time which therapeutic cells are exposed to external perturbation, thus increasing their viability.

Since the microcapsules are all the same size and almost the same net charge, making it difficult to sort, in this study the two sorting techniques which are extensively explored are active electrophoresis (EP) and passive deterministic lateral displacement (DLD). Under *section 1.9 Overview of Sorting*, we look into the importance of combining both the techniques of EP and DLD.

1.8.2 Principle of Electrophoresis

Electrophoresis (EP) is defined by the motion of a charged body in response to an electric field gradient [18]. This movement of the charged particle occurs due to an electrostatic effect driving the charged body towards the oppositely charged electrode. The motion follows Coulomb's law. If the electric field at a particular point is known, the EP force [F] experienced by a charged particle with charge [q] is mathematically represented by,

$$F = q\mathrm{E} \tag{4}$$

Where the electric field E is given by,

$$E = \frac{V}{d} \tag{5}$$

In which,

V- Applied voltage

d- Distance between two electrodes

If the charge [q] at any given time is of positive magnitude, the net force applied would be in the same direction as the field. In the same way, if the charge [q] is of negative magnitude, the applied force would be in the opposite direction, as demonstrated in *Figure 8*.

Combining electrophoresis with microfluidics has shown potential in DNA analysis (gel electrophoresis on chip) [41] and cell sorting [42]. Stokes law demonstrates the force exerted on the movement of particles inside a viscous fluid. During electrophoresis, the force (F) exerted due

to electric field is counteracted by a drag force (F_d) due to the presence of fluid around the particle. This drag force can be expressed as:

$$F_d = 6\pi\mu r V \quad (6)$$

Where,

μ - dynamic viscosity of the fluid

r- radius of the particle

V- Velocity of the particle

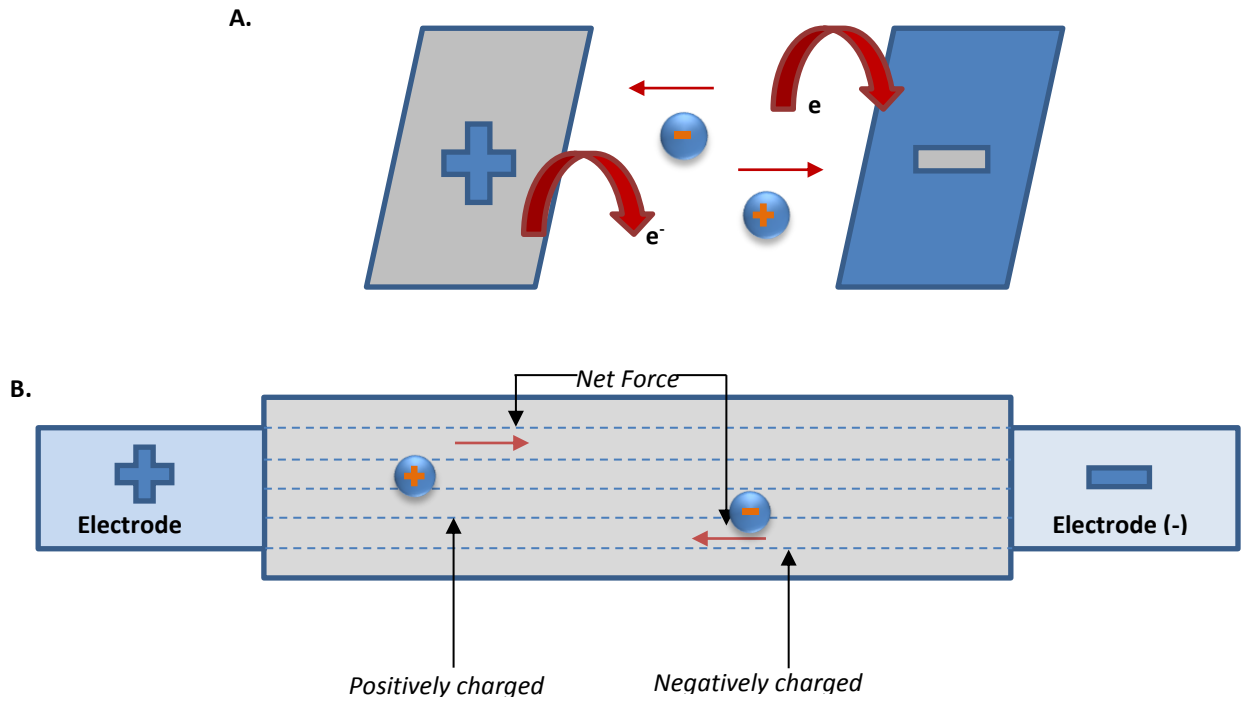

Figure 8 A. Experimental illustration of coulomb's law demonstrating the quantifiable force between two stationary charged particles. B. Demonstrates a similar setting where a particle placed inside a microfluidic channel experiences motion in response to an electric field towards the electrode of opposite charge.

1.8.3 Principle of Deterministic Lateral Displacement

Deterministic lateral displacement (DLD) is a microfluidic sorting technique, first introduced by *Huang et al. 2004*, the technique utilizes specific arrangement of posts (vertical pillars) within a microfluidic channel to control particle movement based on their size and interaction with the posts.

In general, DLD devices take advantage of the asymmetric bifurcation of laminar flow in order to deviate particles into a desired trajectory [43]. To understand the flow regime of a DLD based device, consider a small portion of micro-post array, as seen in *Figure 9B*, where the horizontal and vertical distance between two pillars is denoted by D_x and D_y respectively. In this study, D_x=D_y, and the diameter of pillar is given by D_p. The angular shift between two rows of micro-post array is given by θ. When a sample enters the DLD array, it will collide with these posts and enter a different flow pathway. If a small particle enters the array, it will continue to move around the posts in a '*zig-zag motion*' and resume its original direction upon leaving the DLD array. However, if a bigger particle enters the array, it will get deflected into a different trajectory, wherein the particle will enter a '*displacement mode*'. This displacement or deviation of particles from their original pathway is dictated by the shift θ.

The shift between the 'zig-zag' and 'displacement' modes is dependent upon a factor called critical diameter, D_c. D_c was analytically derived by John Alan Davis in his thesis by fitting the data collected from 20 different devices covering a wide range of horizontal distances D_x ranging from 1.3 µm to 38 µm expressed in equation (7) [44]. In this thesis we adopted the same equation for fabrication and experimentation purposes.

Where,

$$D_c = 1.4G\varepsilon^{0.48} \quad (7)$$

G - (length)

ε= variable parameter equivalent to *tan* θ (degrees)

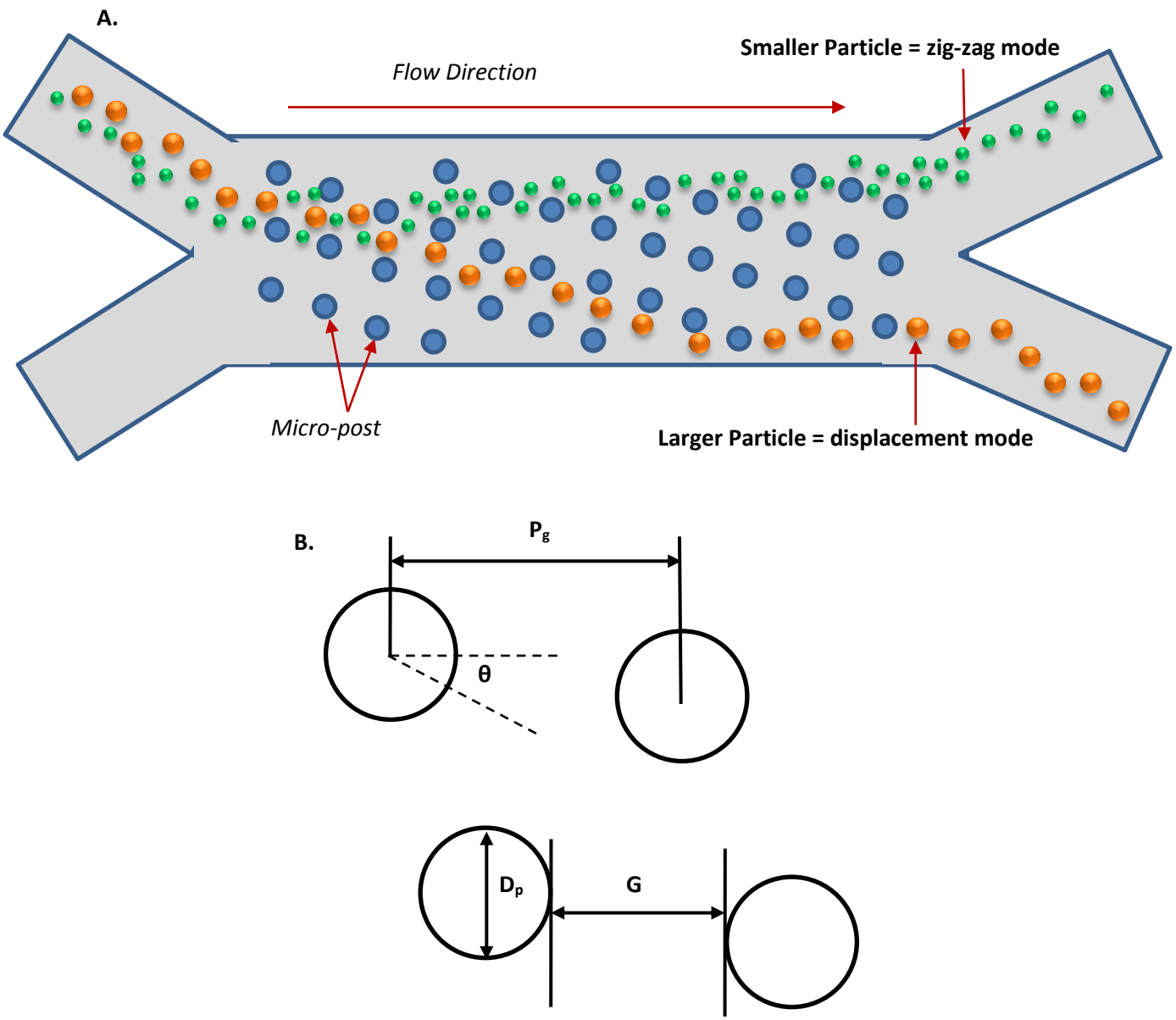

Figure 9 A. DLD array demonstrating the deflection of larger particles in displacement mode, when compared against smaller ones which travel in a zig-zag trajectory. B. A small enlarged section of the DLD array to understand the mechanism of deflection with contributing factors of Pillar Gap (P_g), Lateral Gap (G), Pillar Diameter (D_p) and angle of deflection (ϑ).

1.9 Overview of Sorting

In order to summarize our goals in this study to sort cell-laden microcapsules, three cases with their shortcomings have been presented below,

Ideal Case

An ideal case would be to achieve sorting of empty and occupied microcapsules, wherein each set of microcapsules would exit in a separate outlet. However, all microcapsules (empty and occupied) produced are of similar size and charge, so this case is challenging to achieve.

Figure 10. Ideal case for sorting of empty and occupied microcapsules

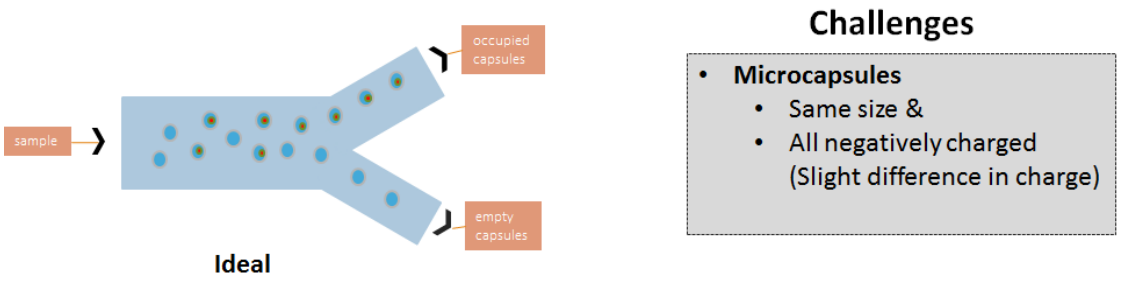

Electrophoresis Sorting

Electrophoresis can be used as a sorting strategy by placing lateral electrodes along a microfluidic setup. As microcapsules display movement in response to charge, they may be deflected into different flow pathways. Since all microcapsules (empty and occupied) are negatively charged, sorting cannot occur solely based on charge deflection.

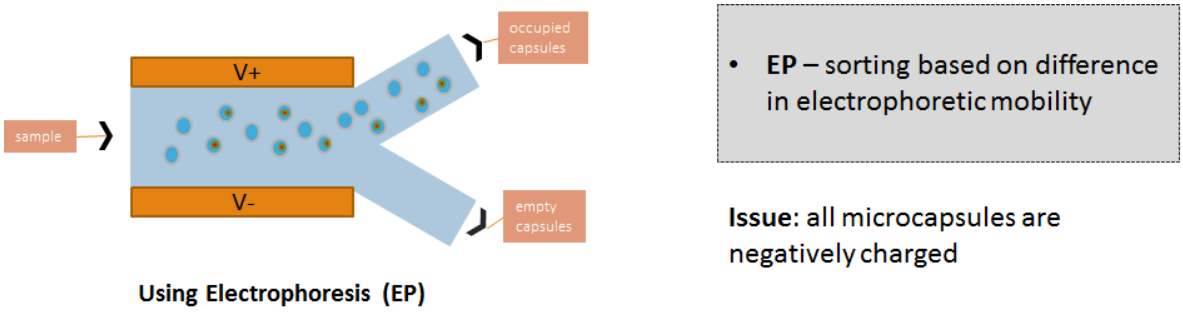

Figure 11. Concept for sorting of microcapsules based solely on EP

Deterministic Lateral Displacement Sorting

The Deterministic Lateral Displacement (DLD) sorting technique uses micro-post arrays inside a microfluidic platform to allow deflection of bigger particles into a separate outlet while allowing smaller ones to run through, discussed in *Section 1.8.3 Principle of DLD*. Since all the microcapsules produced during the encapsulation are of the same size, the technique alone would result in no sorting at all.

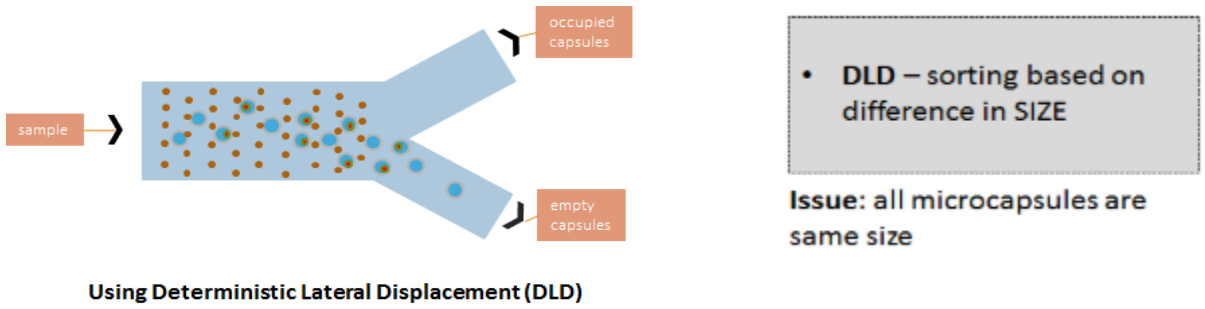

Figure 12. Sorting of microcapsules based solely on DLD

Deterministic Lateral Displacement (DLD)- Electrophoresis (EP) Sorting

Combining the two models of deterministic lateral displacement and electrophoresis, we can control the microcapsule behavior and channel them to a desired pathway. The sorting in our study will be based on occupancy (empty vs. occupied microcapsules). As shown in *Figure 13*, due to DLD all microcapsules will be deflected to a specific pathway, but under the influence of an electric field (EP) we can channel the occupied microcapsules to a different trajectory, based on the difference of their net negative charge.

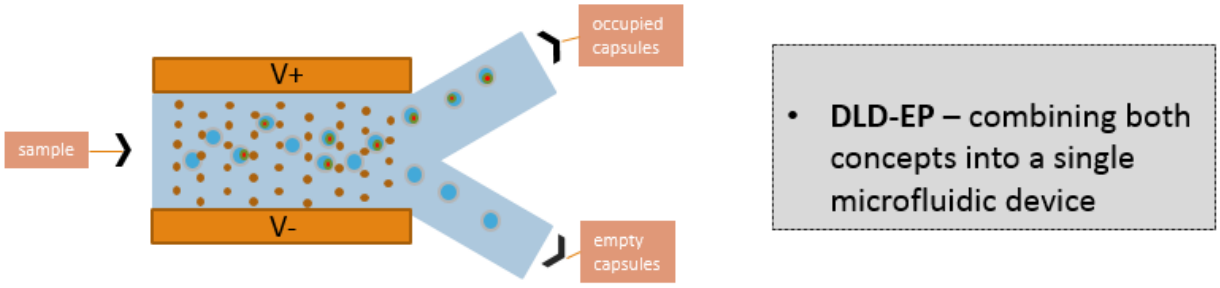

Figure 13. Sorting of microcapsules based on DLD-EP

In the next few sections we look into, a combination of the conceptual takeaways from electrophoresis (EP) and deterministic lateral displacement (DLD) sorting techniques to manipulate agarose based cocoons, encapsulated via droplet based microfluidics, with an overall goal to increase occupancy.

CHAPTER 2

Microcapsule Characterization- Electrophoresis

In this chapter, microcapsules are characterized based on their electrophoretic response. Three variety of microcapsules, namely, cell-laden, polystyrene beads-laden and empty microcapsules are considered to explore their behavior under the influence of a DC electric field.

2.1 Theory

Electrophoresis (EP) refers to the movement of a charged particle inside a fluid based medium, in the presence of an electric field as explained in *section 1.8.2 Principle of EP.* In the past, electrophoresis has shown applications in pathogen detection and biomarker analysis [45]. Due to deflection of charged particles, electrophoresis can be exploited as a sorting mechanism inside a microfluidic channel.

In order to understand the working of electrophoresis in relation to sorting, consider a microfluidic setting; charged particles within an electric field are set into motion towards the opposite charged electrode. The net force exerted on a charged microcapsule is a balance between electrostatic force and hydrodynamic drag. Acceleration upon application of the electric field decreases to zero very quickly when the electrostatic force is equivalent to the hydrodynamic force, resulting in a constant terminal velocity for the particle itself [46]. This terminal velocity ($v_{particle}$) of the particle in motion, is directly dependent on the electrophoretic mobility (μ_{ep} – $m^2s^{-1}V^{-1}$) and the charge density (E) of the particle can be expressed as,

$$v_{particle} = \mu_{ep} E \tag{8}$$

The electrophoretic mobility can also be defined using another equation,

$$\mu_{ep} = \frac{q}{6\pi\mu r} \tag{9}$$

Where,

q = particle charge (Coulomb)

μ = coefficient of viscosity of buffer solution (Pa-s)

r = radius of particle (meters)

Thus, the velocity of the particle is directly proportional to its charge (q). The velocity is calculated by a simple measurement of time required for the microcapsules to travel a known distance [47].

Hydrogel or agarose based microcapsules (created using the technique presented in *section 1.7 Cell Encapsulation technique*) are negatively charged due to the presence of sulphate and pyruvate groups [48]. Cells are mainly negatively charged as well because of membrane based phospholipids [49]. Therefore, it should be noted that cell-laden microcapsules can potentially carry a different net charge compared to empty microcapsules. Of the 55-60 μm microcapsule, the cell occupies roughly 1.3% of the total microcapsule volume, assuming the size of the cell is 14-18 μm.

$$\frac{V_{microcapsule} - V_{cell}}{V_{microcapsule}} \times 100 = 98.7\%$$

where,

$V_{microcapsule}$ = volume of sphere of radius 30 μm for an empty microcapsule

V_{cell} = volume of sphere of radius 7 μm for a cell

Therefore, it may be interesting to observe the difference of net charge caused by the presence of cell inside the microcapsule. This can be achieved through our EP experiments.

2.2 Device Design and Fabrication

In this test device, the microcapsules travel in a single microfluidic channel which consists of a 1 cm 'measurement region' and the particle trajectory is captured here via image acquisition. Two electrodes are introduced within the microchannel, one near the fluidic inlet and the other closer to the outlet, as shown in *Figure 14 B.* The schematic demonstrating how the microcapsules actually travel inside the microfluidic device is shown in *Figure 14 A.*

Electrodes are designed in-lab using a Pt-wire of 0.25 mm diameter (45093, Alfa Aesar) and poly-ethylene sleeve (1.25mm) which is connected to a DC power supply unit. This allows the electric field to cover maximum area around the cross section of the channel.

The device itself is fabricated via soft photolithography which involves a series of steps explained in detail under *Section 1.6.4 Soft-Photolithography.* The actual device bonded on a glass is shown in *Figure 14 B.*

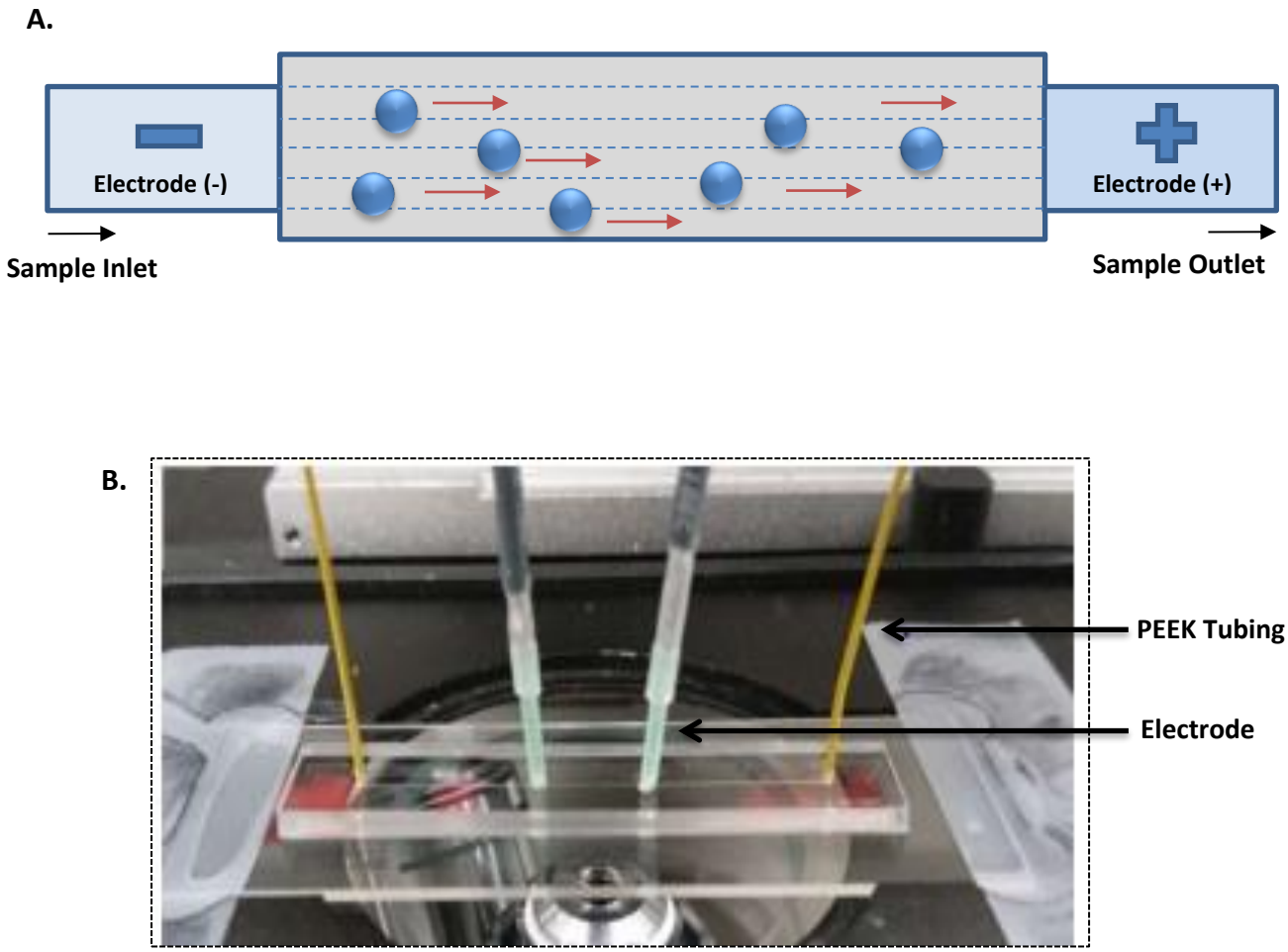

Figure 14 A. Schematic for EP device demonstrating the movement of microcapsules towards the positive electrode as the microcapsules are negatively charged (electrodes encased in GREEN tubing). B. Actual microfluidic platform on a microscope setup ready for experimentation. The sample is stored in a vial which is pressure controlled and delivered to the device via YELLOW peek tubing. The distance between the electrodes is 1 cm, this is also the 'measurement region'.

2.3 Setup

The block diagram setup used for electrophoresis characterization is shown in *Figure 15*. The microfluidic device is placed onto a microscope setup for visual aid.

- **Pneumatic:** microcapsules contained in a vial are pressure driven to the device via peek tubing

- **Image Acquisition:** movement of microcapsules is captured by a camera connected to the microscope
- **Analysis:** videos are analyzed frame-by-frame using the Image-J software on an external computer

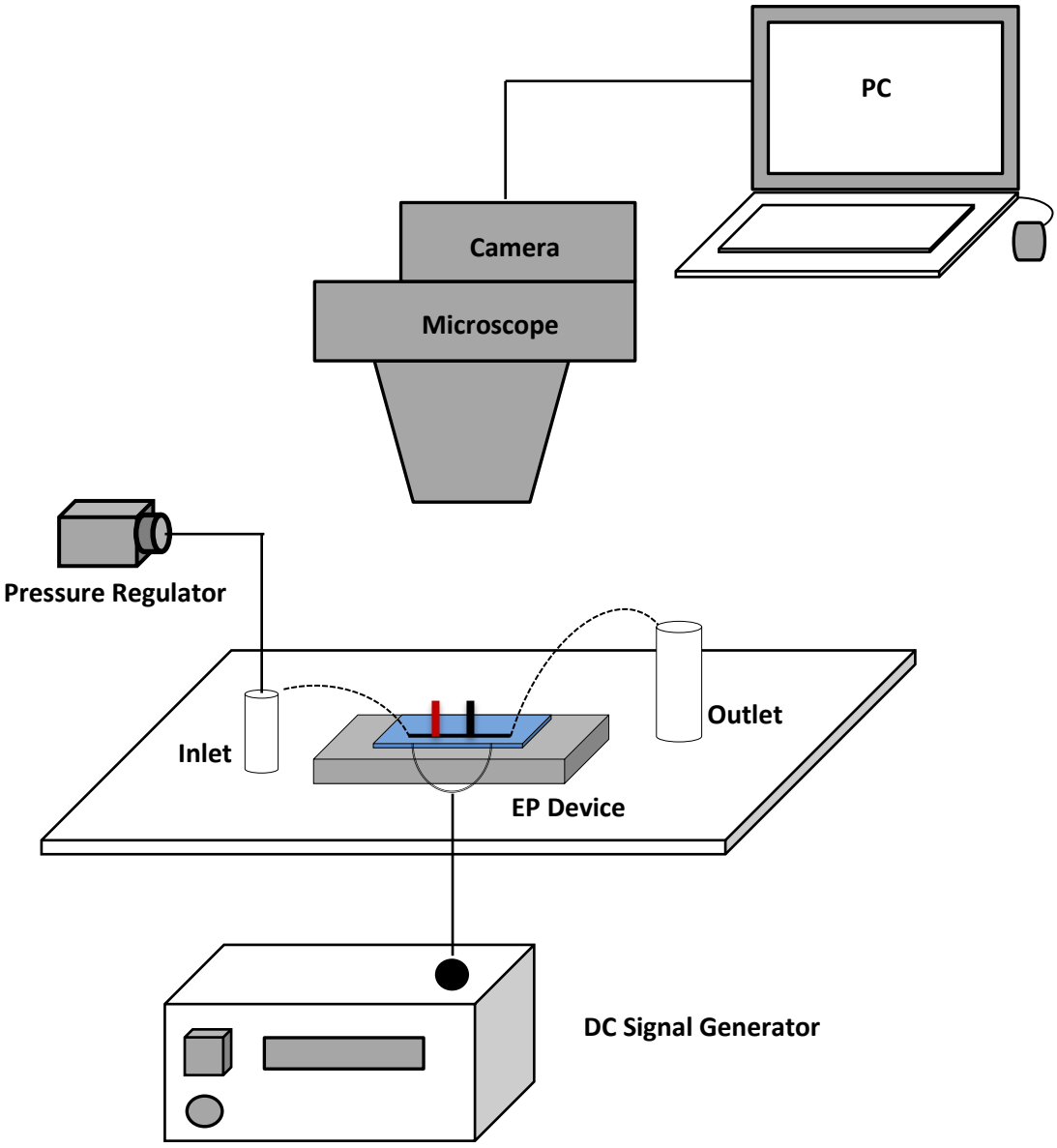

Figure 15. Block diagram for the EP Setup. EP device has a single inlet and outlet with a 1 cm measurement in between. The DC generator is connected via electrode and produces the electric field which is required for the experiment. The microscope is connected to a camera and in turn to an external monitor for real time image acquisition.

2.4 Sample

Samples used for the electrophoresis experiments included agarose microcapsules that were either empty, or contained *NIH-3t3 cells* or polystyrene beads (~11 µm). All microcapsules were spherical with a diameter of 55-60 µm.

Cell-laden microcapsules after the encapsulation process are usually suspended in a cell culturing medium, this media is highly rich in free ions which helps in maintaining the isotonic balance between the inside and outside of the cell, promoting homeostasis [50]. On the other hand, polystyrene beads-laden microcapsules are collected in a desired collection media. For our study, an electric field needs to be applied to the contents encapsulated in microcapsules. It should be noted that applying a high strength electric field to cells in an ion rich media may cause cell death and also corrosion of electrodes via parasitic electrochemical effects. In order to mitigate this, generated microcapsules are suspended in a low-conductivity medium (LCM) solution for the electrophoresis experiments. Even though, LCM is a low isotonic solution, it continues to ensure cell viability [51]. The solution itself is composed of 8.5% sucrose and 0.3% dextrose dissolved in distilled water, maintaining a pH of ~7.

2.5 Quantification

The device is setup as described in section *2.3 Setup* and microcapsules are allowed to flow inside the microfluidic channels till they reach the measurement region. At this point, the pressure regulators of the inlet and outlet (as shown in *Figure 14 A*) are balanced out so that there is no net movement of microcapsules caused due to fluid flow. At this point, the electric field is turned on by applying a voltage difference between the two electrodes.

2.6 Results

2.6.1 EP for Empty vs Cell-laden microcapsules

The goal of EP characterization was to compare the electrophoretic mobility of empty and cell laden microcapsules. It should be noted that the cells continue to maintain their viability throughout the course of the experiments [52][53]. By examining the relative terminal velocity experienced by these set of microcapsules, an ideal condition could be proposed to sort them. All microcapsules tested were of range 55-60 µm in diameter. The EP was measured for electric fields of 50 V/cm, 100 V/cm and 200 V/cm.

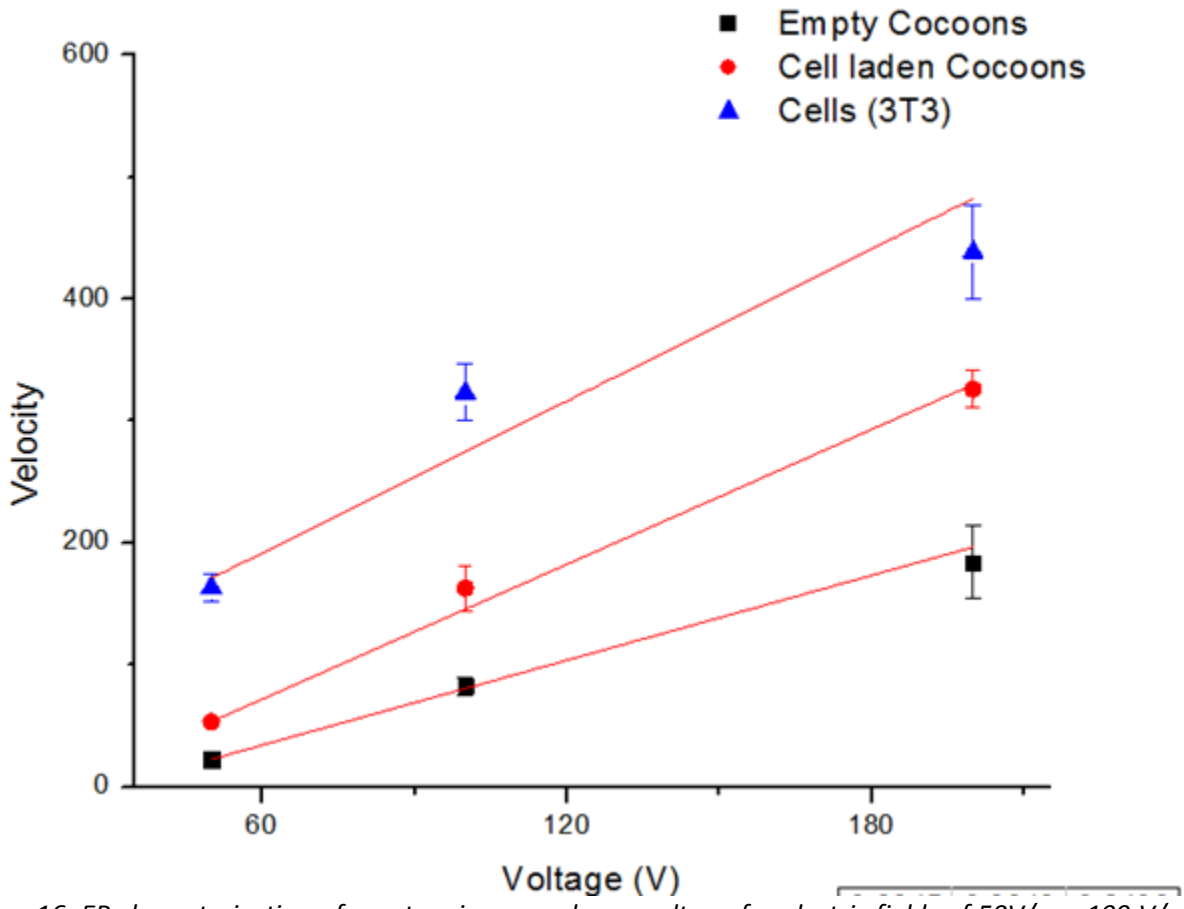

Figure 16. EP characterization of empty microcapsules vs voltage for electric fields of 50V/cm, 100 V/cm and 200 V/cm. Error bars represent the standard deviation of terminal velocity with n=3. The graph was linear fitted for all 3 microcapsules; cells [3T3] y=137.55x + 33.28 R^2=0.858, empty y=81.34x – 65.46 R^2=0.977, cell-laden y=135.6x – 92.2 R^2=0.987. The unit for velocity is µm/s.

As seen in *Figure 16*, the three spectra show a linear response to the various voltages applied and the error bars represent the average of microcapsules at any given point [n=3]. The experiment was repeated more than two times and a significant difference between the sets were observed on each occasion. Both empty and cell-laden microcapsules tend to be negatively charged in nature due to the presence of sulphate/pyruvate [54] groups and phospholipids [55] on their membranes, respectively. Since cells are negatively charged primarily due to membrane based phospholipids [56], once they are introduced inside empty microcapsules, the overall occupied microcapsule may result in a greater net negative charge. The cell-laden microcapsules in our experiments were kept constant at 1-2 cells per microcapsules and this was maintained throughout the study. In *Figure 15*, we notice a trend that cell laden cocoons travel at a faster rate compared to empty cocoons. By comparing the linear fit equation of trends (shown in *Figure 15*) with *Equation 8,* it can be concluded that the slope is equivalent to the electrophoretic mobility (μ_{ep}). By using the value of μ_{ep} and radius (r) in *equation 9*, we can calculate the net charge of various microcapsules as shown in *Table 1*.

Particle	**Radius (µm)**	**Charge (10^{-11} Coulombs)**	**Electrophoretic Mobility ($10^{-4}cm^2$ /V-s)**
Cells	7	1.81	137.55
Empty Microcapsule	30	4.60	81.34
Cell-laden Microcapsule	30	7.37	136.77

Table 1 Net charge and Electrophoretic mobility for cells, empty microcapsules and cell-laden microcapsule.

Therefore, from the data acquired through comparison, we can say that the presence of cells inside an agarose microcapsule significantly increases the electrophoretic mobility as shown in *Table 1*. With that said, it is fair to assume that due to the higher charge concentration of cells, when they are embedded into an empty microcapsule, the resulting occupied microcapsule shows a higher net charge.

2.6.2 EP for Empty vs polystyrene beads-laden microcapsules

The cells were substituted with polystyrene beads (1-2 beads per microcapsule) of size ~11 µm and the size of microcapsules was maintained at 55-60 µm in diameter. Polystyrene beads serve as a good substitute for cells as it simplifies the experiments providing ease of encapsulation, being a synthetic model. Since the surface of polystyrene beads are generally coated, being either positive or negative [57] in order to avoid coalescence, the core of the beads however, remain neutral. Therefore, due to the presence of neutral charge, the net negative charge of polystyrene beads microcapsules may be lower than empty microcapsules (less negative).

Measurements were taken for electric fields of 100 V/cm, 200 V/cm, 300 V/cm and 400 V/cm. The goal of these experiments was to notice a significant difference in electrophoretic mobility between the empty and polystyrene beads-laden microcapsules.

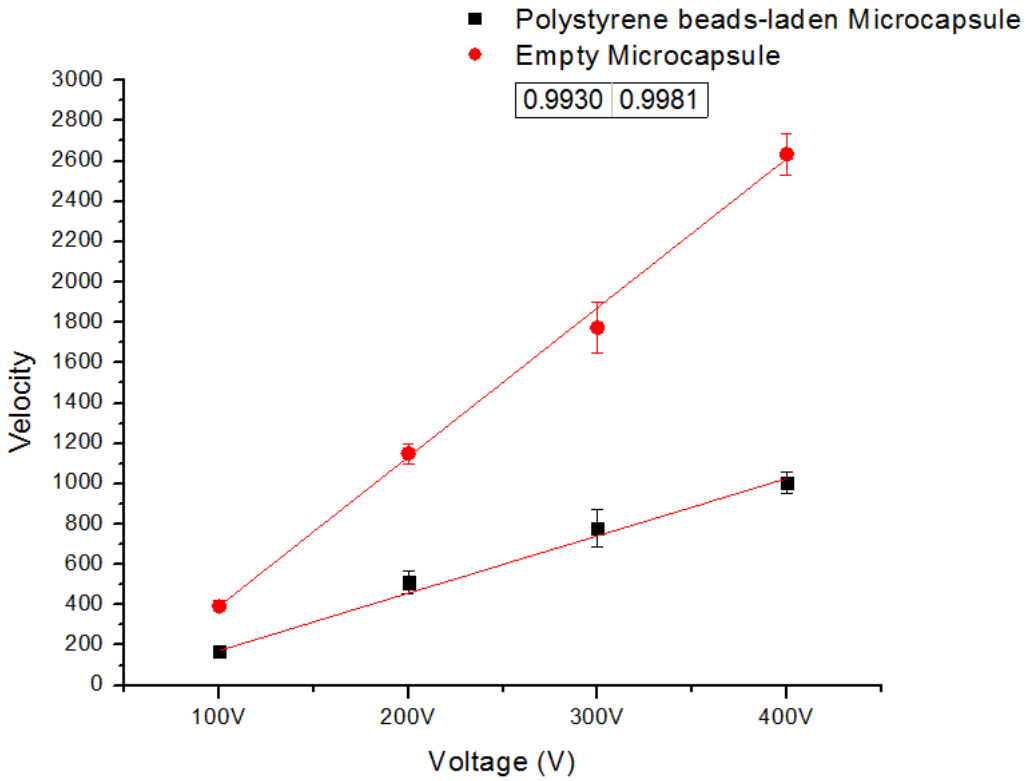

Figure 17. EP characterization of empty microcapsules vs beads-laden microcapsules for electric fields of 100 V/cm, 200 V/cm, 300 V/cm and 400 V/cm. Error bars represent the standard deviation of terminal velocity with n=3. The unit for velocity is µm/s.

Two linear spectra were observed with error bars representing an average of microcapsules at any given point [n=3]. Experiments were performed 3 different times with significant difference observed in each set. Empty and beads-laden microcapsules both showed a negative charge response to the electric field applied. It may be inferred from the results that empty microcapsules travel faster than polystyrene beads-laden microcapsules, which can be expected, as polystyrene beads attached to agarose capsules decrease the net charge of the microcapsules by occupying space within the hydrogel network.

2.7 Discussion

With EP characterization, we were able to understand the behavior of empty, cell-laden and beads-laden microcapsules under an applied electric field. To summarize, a significant difference in the terminal velocity was observed between empty and cell-laden microcapsule, which is indicative of the fact that the presence of cells inside an agarose based capsule increases the net electrophoretic charge. An opposite trend was seen for polystyrene beads-laden microcapsules, as they were slower than empty ones. The choice of collection media in which the microcapsules are collected can affect the results obtained through EP. Replacing the cell culture media with LCM helped in avoiding complications such as apoptosis of cell and any damage to the electrodes. However, poor conductivity can cause field distortion (polarization) resulting in an uneven electric field around the electrodes. Therefore, in order to measure mobility, small amount of conductivity/salt is required [58]. For our EP recordings, another detail that was witnessed is the fluctuation between the terminal velocities across a set of experiments. This can be justified due to the variation of the presence of salt during different set of experiments. During encapsulation of cell-laden microcapsules, we try to remove cell culture media at the initial steps through filtration by using centrifugation. There is a possibility of few free-ions being released into the collection media which can cause variation in results. Another logical reasoning could be due to batch variation of agarose as experiments for polystyrene-bead-laden microcapsules were performed at later stages. Nonetheless, we can ensure that for a given experiment, conditions are stable enough to uncover different mobility.

After careful examination of the electrophoresis process, one limitation which remains is that, if we were to use two lateral electrodes alongside a microfluidic setup as shown in Section *3.5.2 Electrophoresis Sorting*, both empty and occupied (cell-laden and polystyrene beads-laden) microcapsules would travel in a similar trajectory. The reason for this being, even though they show a significant difference in their EP characteristics, both empty and occupied microcapsules are negatively charged.

Nonetheless, the slight differences in their electrophoretic mobility may be applied towards adopting a new sorting technique, combining electrophoresis with Deterministic Lateral Displacement (DLD).

CHAPTER 3

Deterministic Lateral Displacement (DLD)

Deterministic Lateral Displacement (DLD) is a hydrodynamic technique used to separate particles based on the difference in their size. In this chapter, fabrication assembly for the DLD devices was designed and tested with agarose based microcapsules. Furthermore, a variation of device geometries was tested with microcapsules for a proof of concept.

3.1 Theory

DLD has been identified as a high resolution, label-free, passive sorting technique [59]. A recent study based on DLD sorting was used to differentiate non-viable mammalian cells from living ones. The sorting strategy was applicable as cells which undergo apoptosis decrease in size when compared to viable ones [60]. Another study demonstrated the ability of DLD to sort leukocyte subpopulations (T-lymphocytes and neutrophils) from a blood sample by using the concepts of cell size and deformability [61]. However, both studies used polystyrene microspheres as proof of concept for validating their sorting device.

Conceptually, DLD leverages laminar flow and passive sorting techniques for particle deflection. In a microfluidic setting, due to the small channel geometry, the Reynold's number is often less than 1 (as discussed in *Section 1.2 Microfluidics*), which suggests a laminar flow regime in the microchannel. Assuming there is no slippage between solid phase (e.g. microcapsule particles) and the adjacent flow streamlines, in a straight channel, the particles will move in straight paths parallel to streamlines. In order to deviate the particle flow pathway, there is a need to insert obstacles or pillars inside the channel. In DLD method, an array of microscale obstacles or pillars are used to assign particles into exclusive streamline pathways based on their size. The separation between the pillars is largely dependent upon the critical diameter (D_c) of the DLD device which has been discussed previously under *section 1.8.3 Principle of DLD.*

3.2 Design and Fabrication

3.2.1 Design

The design of DLD devices requires an array of pillars within a microfluidic channel. *Figure 18* shows a representative building block of such pillar arrays. The device layout was designed through AutoCAD®and can be divided into three sections as shown in *Figure 19*,

- **Inlets**
  - $Inlet_1$: inflow of sample
  - $Inlet_2$: inflow of buffer *(will be discussed in Chapter 4)*
- **DLD Array**: comprises of micro-scale pillars and primary deflection region
- **Outlets**
  - $Outlet_1$: undeflected sample collection
  - $Outlet_2$: deflected sample collection

The pillar diameter (D_p), pillar gap (P_g) and critical diameter (D_c) are crucial factors to achieve particle deflection as shown in *Figure 18*.

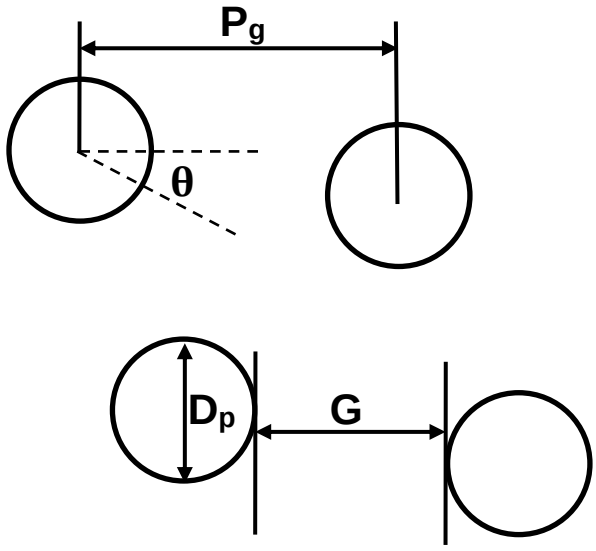

Figure 18. Cross-section top view of DLD array depicting individual micro-post pillars, where D_p is pillar diameter, P_g is pillar gap which is the distance from center-to-center of two adjacent pillars and G is the lateral gap or end-to-end distance between two adjacent pillar.

In this study, we chose D_p = 70 um, P_g = 170 µm. Subsequently, Lateral gap (G) = 100 µm *(=170 µm - [radius of two pillars])*. Critical diameter (D_c) from *equation 7* is dependent upon the lateral gap (G - length) between two pillars and angular shift (ε=tanθ - degrees) [62],

$$D_c = 1.4G\varepsilon^{0.48} \quad (7)$$

The angular shift for the DLD array was set at 5°, chosen so that any particle coming into the top inlet ($Inlet_1$) will be deflected towards the outlet at the bottom ($Outlet_2$) of the microfluidic channel. The critical diameter (D_c) for the device is then formulated out using *equation 7* to be ~45 µm. Based on this information, we predict that microcapsules sized below 45 µm will follow a '*zig-zag*' motion following pillars arrangements in the microchannel, whereas larger microcapsules would fall into the *DLD mode*. The width and length of the microfluidic channel is 2300 µm and 2.5 cm, respectively, and the microcapsules used for experimentation measured 55-60 µm in diameter, i.e. larger than D_c=45 µm.

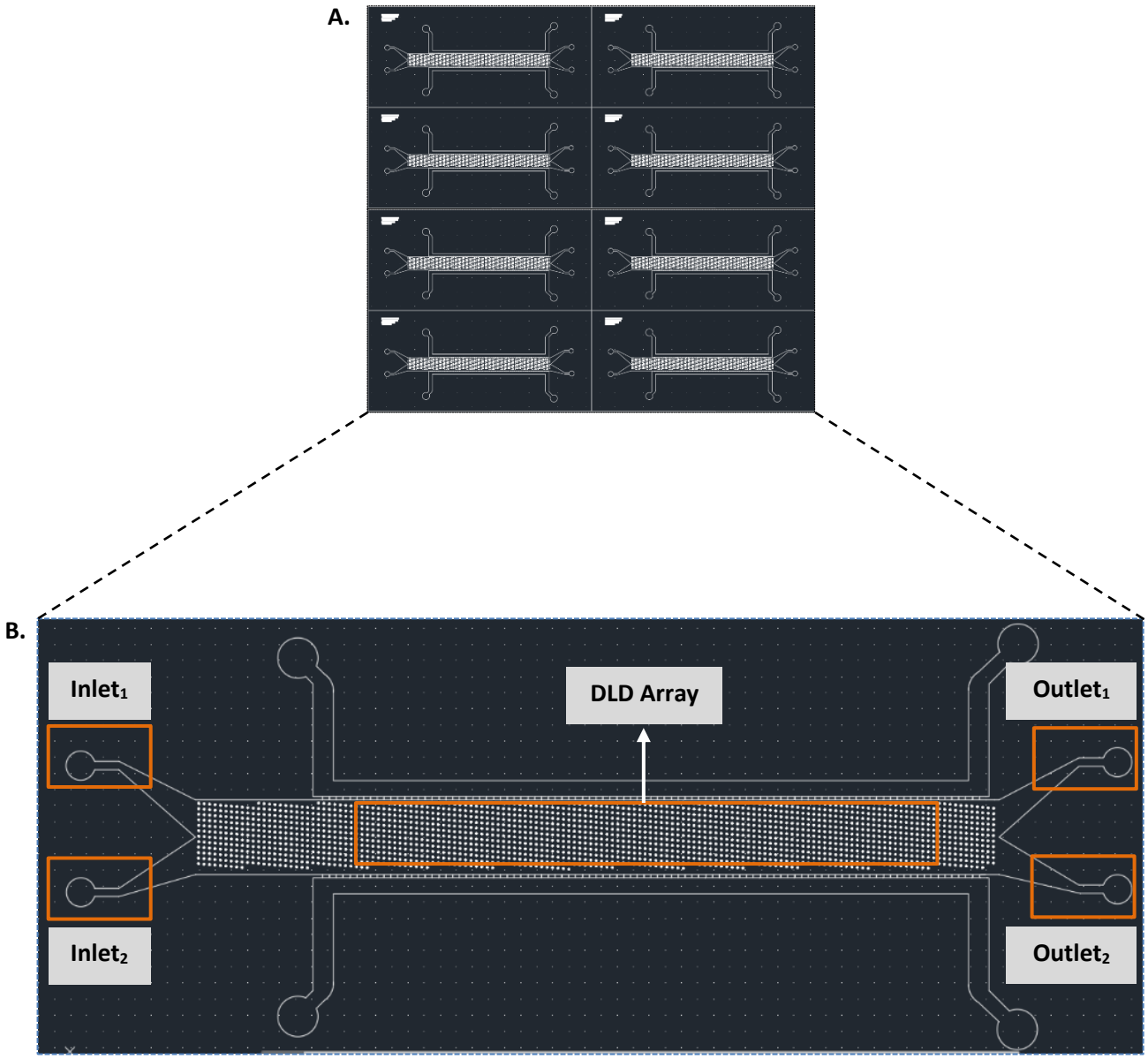

Figure 19 A. Photomask design of DLD microfluidic device B. DLD microfluidic device with regions; Intet$_1$ for sample inflow, Inlet$_2$ for inflow of buffer, middle DLD micro-post array region which consists of pillars for microcapsule deflection, Outlet$_1$ for undeflected sample collected and Outlet$_2$ for deflected sample collection.

3.2.2 Fabrication

Fabricating guidelines for DLD devices has been discussed in detail under *section 1.6.4 Soft-Photolithography* [33]. Briefly, slight variations in pre-bake, exposure, post-bake and revolutions per minute for spin-coater were made to adjust the channel height, as shown in *Table 2*.

Procedure	Detail	Duration
Pre-Bake	The height of the DLD channels was set at 100µm	5 minutes at 65 °C and 20 minutes at 95°C
Spin-Coating	A gradual increase in revolutions per minute was applied. Even spreading of the photoresist (SU-8-2050) aids in maintaining a good contact during exposure to avoid any loss in the resolution [63], which is an essential step to attain minute pillar features.	10 seconds at 500 rpm, 30 seconds at 1500 rpm and 10 seconds at 700 rpm
Exposure	UV exposure was applied to imprint the photomask designs of DLD devices onto the Silicon wafer with SU-8-2050 photoresist.	Exposure time of 14 seconds
Post Bake	Durations adjusted to achieve set microfluidic channel height	5 minutes at 65 °C and 10 minutes at 95°C

Table 2. Summary of adjustments made to fabricate DLD pillar arrays. Fabrication of master mold was followed by Development and Silane treatment stages.

The DLD devices were then casted with PDMS as shown in *Figure 20* and later bonded to a glass slide using the same process described under *Sections 1.6.4 Casting & Bonding.*

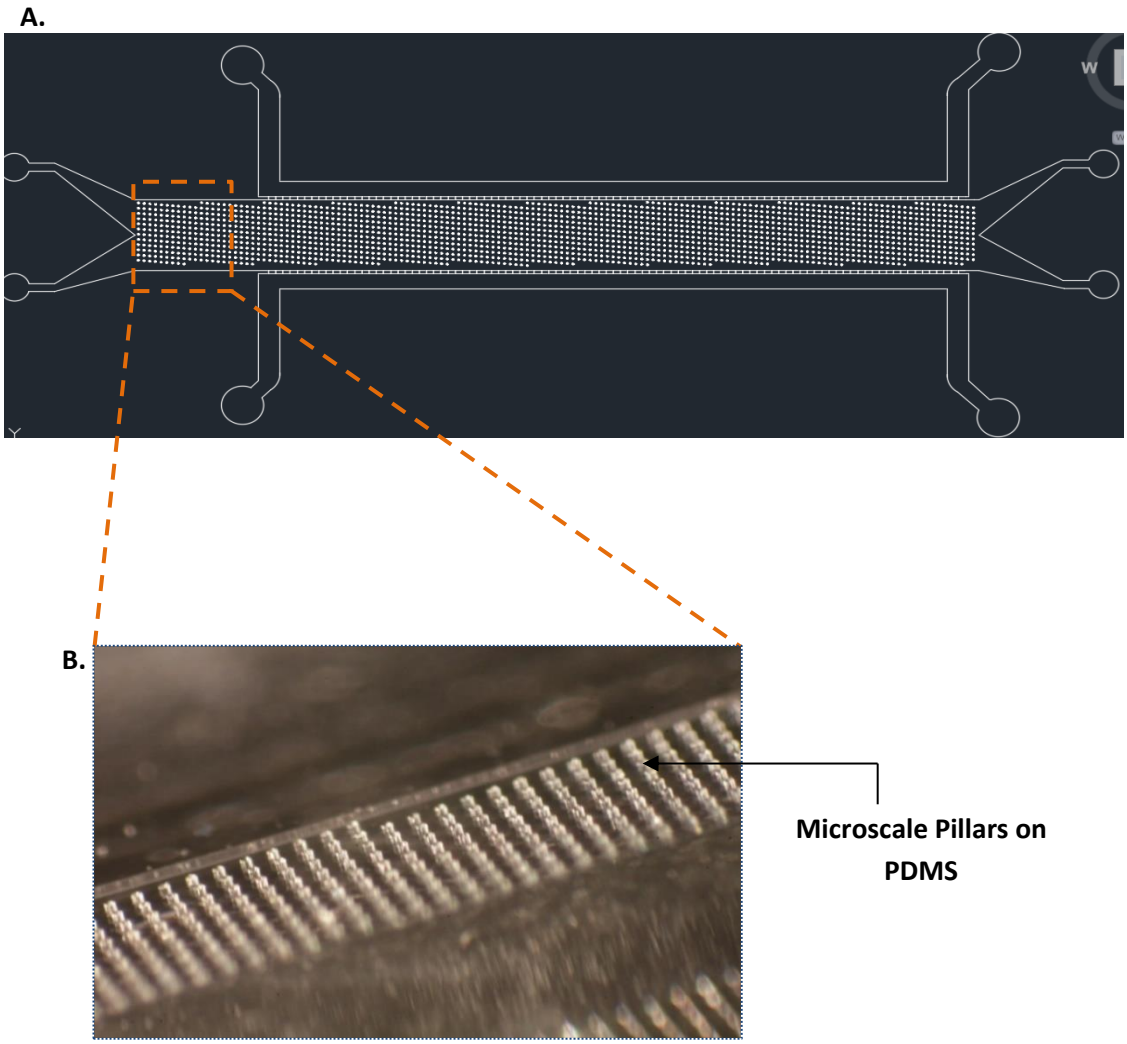

Figure 20. A) AutoCAD blueprint of micro-post pillar design on chip. B) Fabricated PDMS based DLD Devices with micro-scale pillars comprising of a 5 degree angular shift throughout the microfluidic channel, height of pillars aimed at 100µm.

3.3 Proof of Concept

To test out the deflection behavior of the DLD device, microcapsules of range 55-60 µm were introduced into the pillar array at flow rate set through balancing the pressure regulators. Flow rate for this particular experiment was selected on the basis of what is best for visualization under the microscope. Since the size of microcapsules were greater than the critical diameter (D_c) of the device, all microcapsules were averted into a streamline direction from Inlet $_1$ to Outlet $_2$ (checked through video analysis).

Post fabrication showed small variations in dimensions of pillar diameter (D_p) and pillar gap (P_g). The pillar diameters showed a reduction in size (~10-12% deviation from the actual device design) which was determined through imaging analysis (*Image-J software*). To account for these variations, multiple combinations (63/190 µm, 80/220 µm, 70/170 µm and 100/240 µm) of pillar diameter and pillar gap were experimentally tested. However, the D_p and P_g of 70/170 µm validated experimentally, satisfied the ~10-12% reduction acceptance criteria and the microcapsules deflected across the channel as demonstrated in *Figure 21*. Image acquisition was performed by capturing videos using the Point-Grey software.

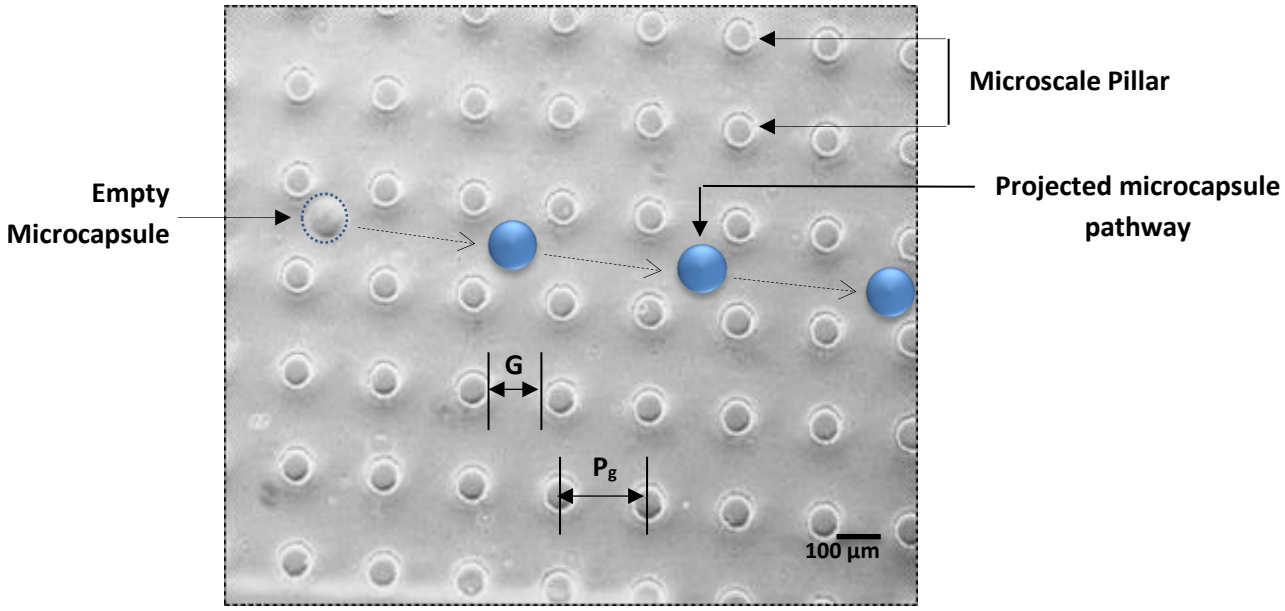

Figure 21. The streamline orientation and depiction of the basic principle of DLD deflection without an external force which in our case is the electric field. An empty microcapsule entering the DLD array (region of video capture) and its projected movement across the channel. The microcapsule is deflected because of the pillars in the channel which are positioned at an overall 5 degree angular shift so as to achieve projected movement. The pillars are sized based on the Lateral Gap (G) which is the end to end distance between two adjacent pillars and the Pillar Gap (P_g) which is the distance between two diameters of adjacent pillars. The diameter of the pillar (D_p) and Pillar Gap (P_g) is set to 70/170 µm.

In the next chapter, we explore sorting as a part of the DLD mechanism. The deflection of microcapsules will be subjected to an external electric field generated by two parallel lateral electrode with the microfluidic channel running in between them.

CHAPTER 4

Combining DLD and EP

To achieve better sorting capability of microcapsules, two lateral electrodes are integrated with the microchannel so that the DLD effect is combined with the gradient of the lateral electrodes, i.e. along the width direction of the microchannel. DLD alone is incapable of sorting unoccupied from occupied microcapsules given that they both have similar sizes. And while EP can deflect the two microcapsule types differently given their slightly differing electrophoretic mobility, sorting remains challenging in practice as all microcapsules are negatively charged overall. DLD is used in concert with EP to provide an 'offset' to the lateral displacement of the microcapsules in order to better facilitate their routing into distinct outlet micro-channels. Three different types of microcapsules, namely, cell-laden, polystyrene beads-laden and empty microcapsules are considered to explore their behavior under the influence of a lateral electric field inside a DLD microfluidic array system.

4.1 Methodology

DLD and EP principles were investigated individually in *Chapters 2 and 3.* In Chapter 2, characterization of a sample of microcapsules; agarose (empty), cell-laden (occupied) or polystyrene beads-laden (occupied) was performed based on their behavior under the influence of a DC electric field in an electrophoresis based microfluidic setting as depicted in *Figure 14*. Results acquired through EP experiments demonstrated that even though all microcapsules (empty and occupied) are negatively charged, they have a slight difference in their net terminal velocities when subjected to EP force. In *Chapter 3*, a DLD array was designed and fabricated to successfully demonstrate the size-based deflection of microcapsules (irrespective of them being empty or occupied).

In this chapter, we combine forces of DLD array and EP to manipulate these microcapsules within microfluidic channels to achieve higher sorting capabilities.

Since experimentation with live cells is highly variable, to avoid complications and for experimental simplicity, a similar model of polystyrene beads is used to replace cells in microcapsules. Through an electrophoresis setup, it was confirmed that agarose capsules containing polystyrene beads travel at a slower speed compared to empty microcapsules as shown in *section 2.6.2 EP for Empty vs polystyrene beads-laden microcapsules.* However, they both have the same size. Therefore, by using micro-post arrays, the goal is to achieve a noticeable difference between the two models (as shown in *Figure 22 B*) and control them with a common variable factor, called as 'Deviation Angle' or the angle between deviation and deflection of microcapsules under the DLD-EP conditions, explained more in detail later in *Section 4.5.1 Characterization of Empty vs Polystyrene Beads Microcapsules in DLD-EP.*

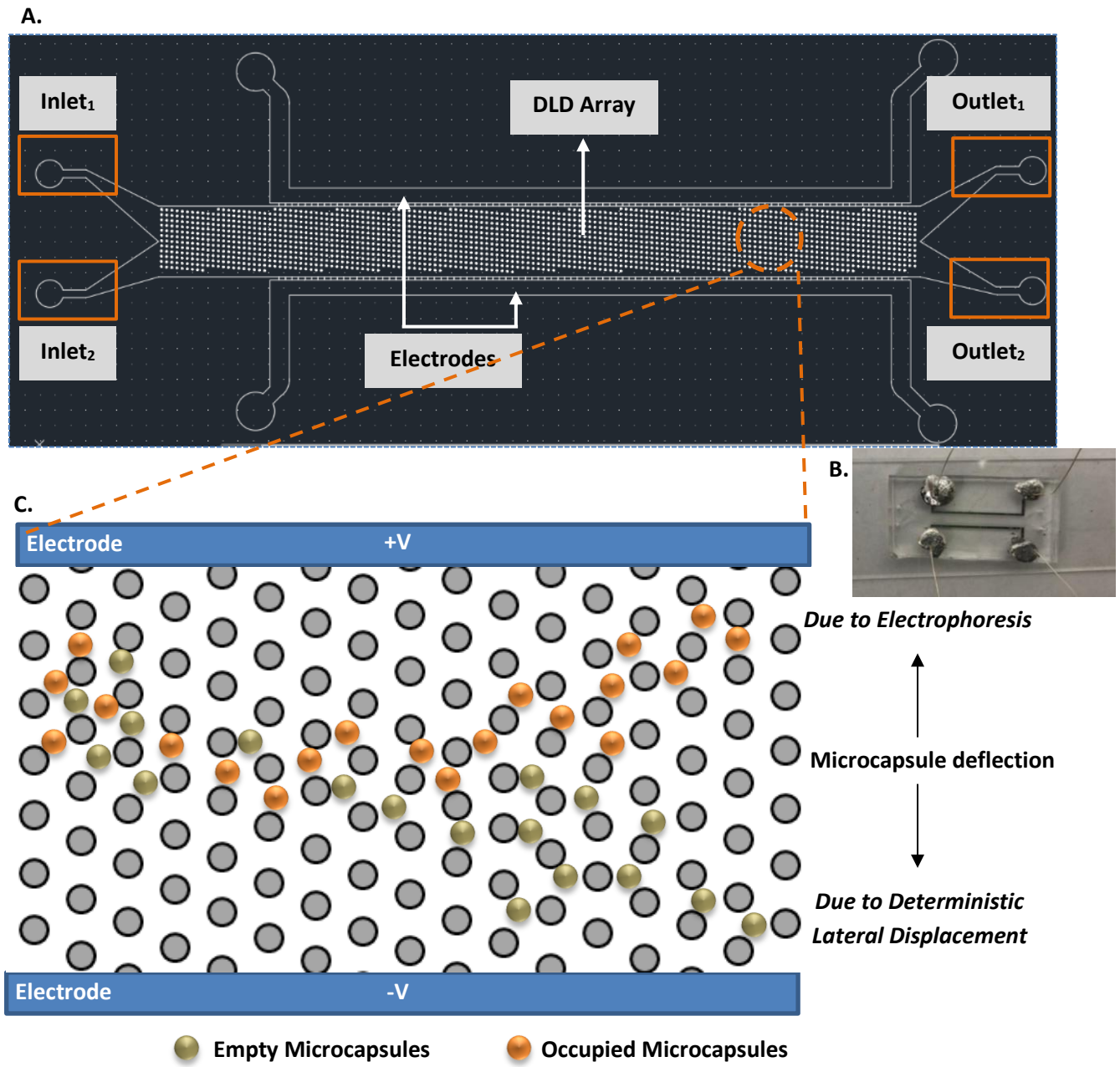

Figure 22 A. AutoCAD drawing of the microfluidic device used for DLD-EP experiments. B. Actual microfluidic device, post fabrication with electrode placed laterally across the DLD region of microfluidic device. C. Flow of microcapsules (empty and occupied cell-laden) beginning from Inlet$_1$ position at the top left corner travelling across the channel and ultimately undergoing deflection. All microcapsules travel towards Outlet$_2$ due to deterministic lateral displacement (DLD, however due to the difference in the net EP shown in Chapter 2, occupied microcapsules travel to Outlet$_1$.

4.2 Electrode Integration and Assembly

Design Layouts and fabrication assembly for DLD devices have already been discussed in the previous chapter. In this section, the DLD array will be sandwiched between two lateral electrode channels which are filled with a bismuth-based low melt alloy (*Roto281F*). Tunnels (10 µm) as shown in *Figure 22 A* are used to link electrodes to the microfluidic channel allowing the electric field to propagate through channel width, bridging from one electrode to the other one.

To fill up the electrode channels, crushed fragments of the low melt alloy ingot were loaded into a 15 mL syringe. The alloy is solid at room temperature but melts at 70 °C. In order to initiate the melting process, the syringe, loaded with the alloy, is kept inside a 70 °C oven. Upon melting the alloy, the syringe is interfaced with the inlet of the lateral electrode channels through plastic tubing. In a matter of a few minutes, the liquid alloy flows through and fills the lateral channels. The same process is repeated for the second lateral channel. The device is then taken out of the oven and this is immediately followed by insertion of silver wires in the lateral channels filled with molten alloy. Upon cooling down of the device the alloy solidifies around the silver wire. A DC power supply unit is used to apply voltage difference across the electrodes to induce EP. The workflow for electrode integration and assembly is shown in *Figure 23*.

A.

B.

C.

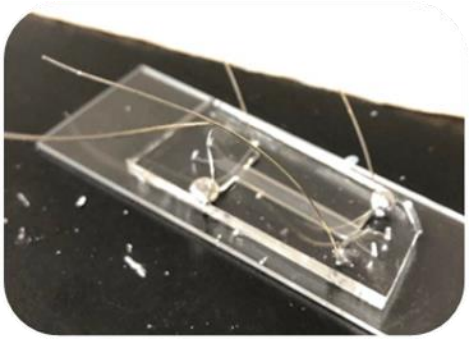

D.

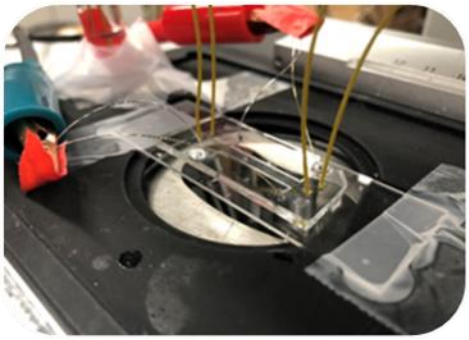

Figure 23. An overview of the entire electrode integration process. A. Solid bismuth based alloy B. The alloy is broken down into smaller pieces and liquid injected onto electrode positions on the microfluidic device inside the oven at 70 °C. C. Insertion of silver wires on the microfluidic device allows connection of the electrodes to an external DC power supply. D. The finished microfluidic device setup

4.3 Setup

The test setup used for DLD-EP experiments is schematically shown in *Figure 24*. The microfluidic device (shown in *Figure 23 C*) setup has 4 components:

- **Pneumatic:** microcapsules contained in a vial are pressure driven to the device via peek tubing into $Inlet_1$, buffer (LCM) stored inside a separate vial is pressure driven to $Inlet_2$ to ensure that all microcapsules maintain a consistent flow gradient at $Intlet_1$.
- **Image Acquisition:** movement of microcapsules inside the DLD array is captured by a camera mounted on the microscope and interfaced with a computer.
- **DLD-EP Device:** microfluidic region of experimentation
- **Analysis:** videos (60 fps) are analyzed frame-by-frame using the Image-J software on an external computer in order to characterize the deflection/movement of microcapsules.

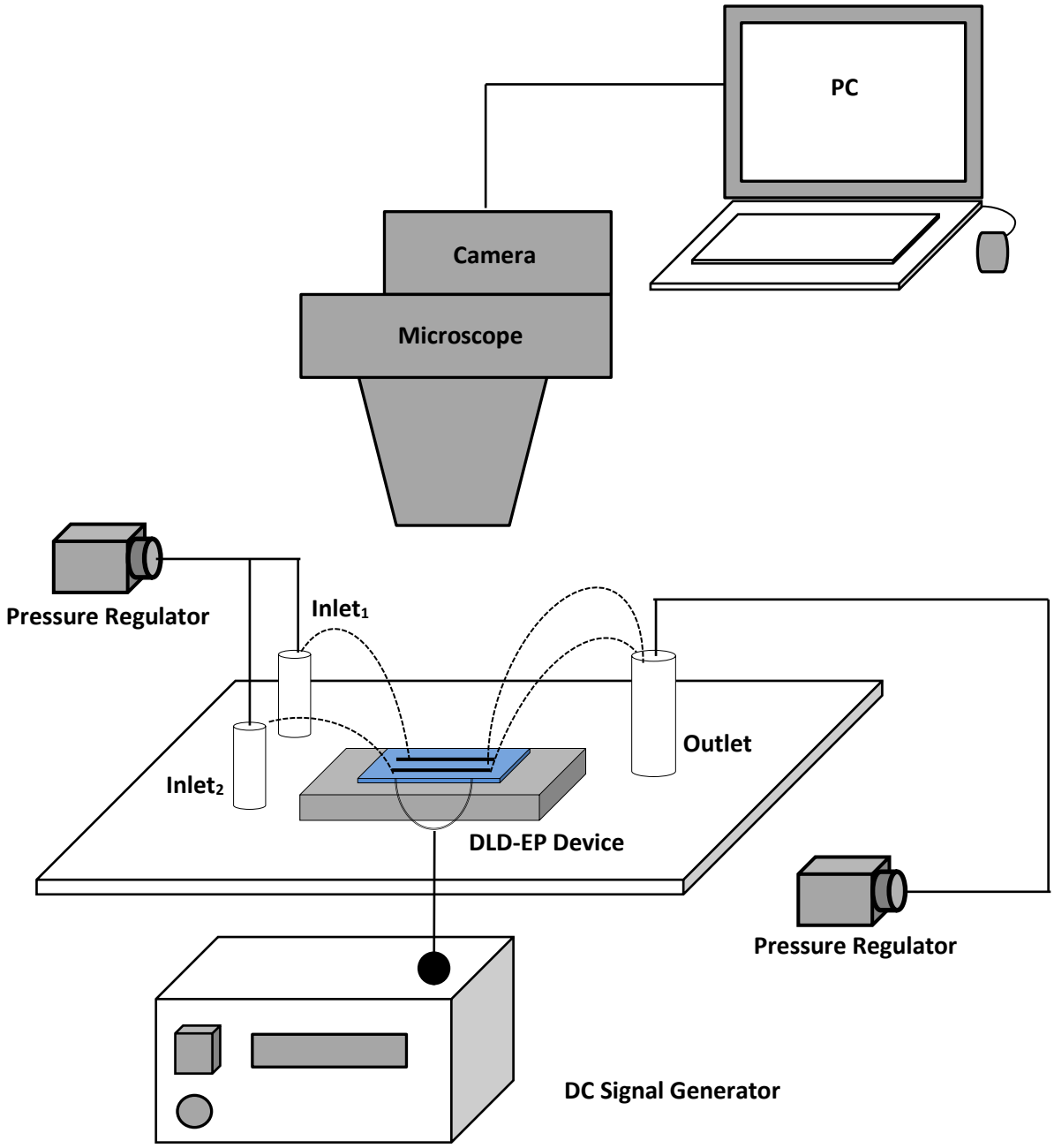

Figure 24. Block diagram for DLD-EP Setup, the microfluidic device is placed onto a microscope setup for which is connected to an external computer. Inlets and outlets are connected with pressure regulators to maintain a desired flow rate inside the channels. A DC power supply unit is connected to the electrodes to supply desired electric field.

4.4 Quantification

Sample of microcapsules (mixture of empty and occupied ones) are introduced into the DLD array through $Inlet_1$ at a set flow rate. The flow rate is manually controlled by pressure-controlled regulators. All microcapsules were suspended in an LCM solution and sized between 55-60 µm in diameter.

As a proof of principle, empty microcapsules were visualized under a section of the device. This section of the device visible under the microscope includes a fraction of the microchannel containing 20 vertical columns of pillars. Motion of microcapsules deflected across this section was visualized under no electric field. Then, at a specific point (the 10th pillar column, or half way through the visual window), the electric field was turned 'ON'. The microcapsules shifted their direction in response to the voltage applied, therefore, deviating from their original pathway (Red arrows in *Figure 25*). The 'deviation angle' was then calculated as the angle between the original pathway under no electric field and the microcapsule flow pathway under an applied electric field, as shown in *Figure 25*.

Further as per our design criteria, Reynold's number was calculated for a static pressure difference of 1 psi. Using equation (1) ($Re = \frac{\rho V L}{\mu}$),

ρ = density of the fluid = 1 Kg/m^3,

V = velocity of the fluid = 117 m/s [$V^2 = 2(P_1 - P_2)$] ,

µ = viscosity of fluid = 1 Ns/m^2,

L = length or diameter of the fluid = 0.0001 m,

With this, Re = 0.0117 resulting in a laminar flow (since Re<< 1)

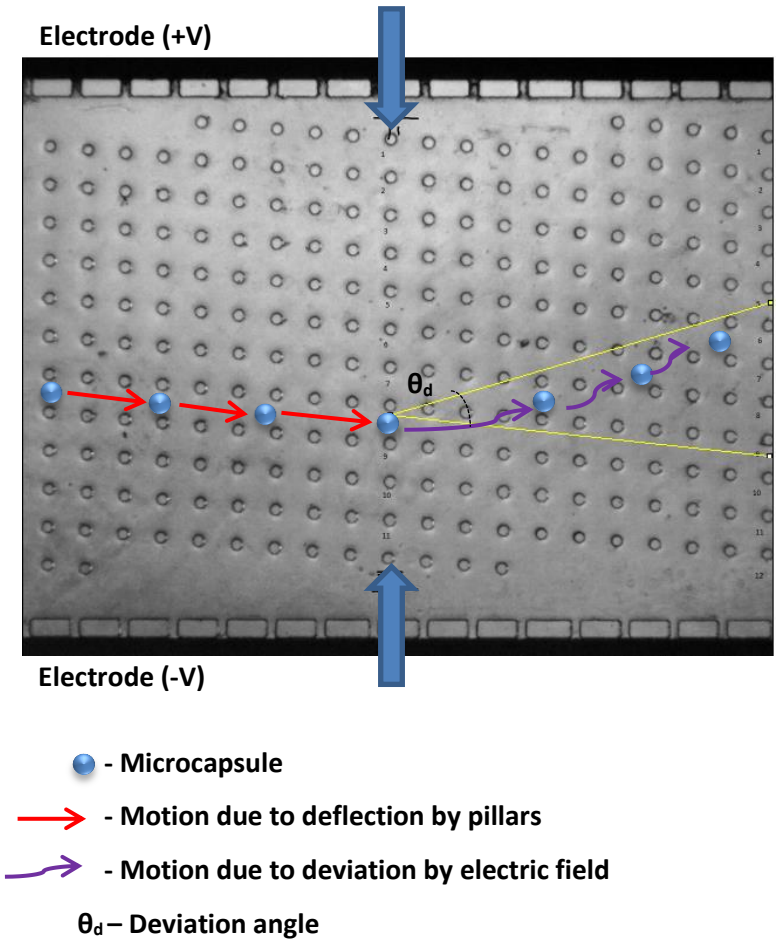

Figure 25. Projected movement of microcapsules (denoted by blue circles) inside the microfluidic channel in accordance with micro-post pillars. The microcapsules are seen to be deflected inside a section of the DLD-EP device. There are two pathways which the microcapsule may follow; 1. Pathway created due to deflection by the micro-post pillars, which is due to DLD and denoted by the red arrows in the figure. 2. Pathway created due to deviation by the electric field which is due to EP, denoted by the purple arrows in the figure. The angle created between these two pathways is called deviation angle (θ_d).

4.5 Proof of Principle

Agarose microcapsules (empty) sized 55-60 µm in diameter were introduced into the DLD array at a constant flow rate. Microcapsules were suspended in an LCM solution.

Under no electric field, when a section of DLD array was visualized under the microscope, the microcapsules were deflected due to the presence of pillars. As the microcapsules continued to deflect across the channel, at the halfway point, an electric field was turned 'ON'. Due to the voltage applied, the microcapsules deviated from their original pathway. This response was noted for various DC voltage values between 15 and 45 V. From this, the deviation angle (θ_d) was calculated after video acquisition and analysis.

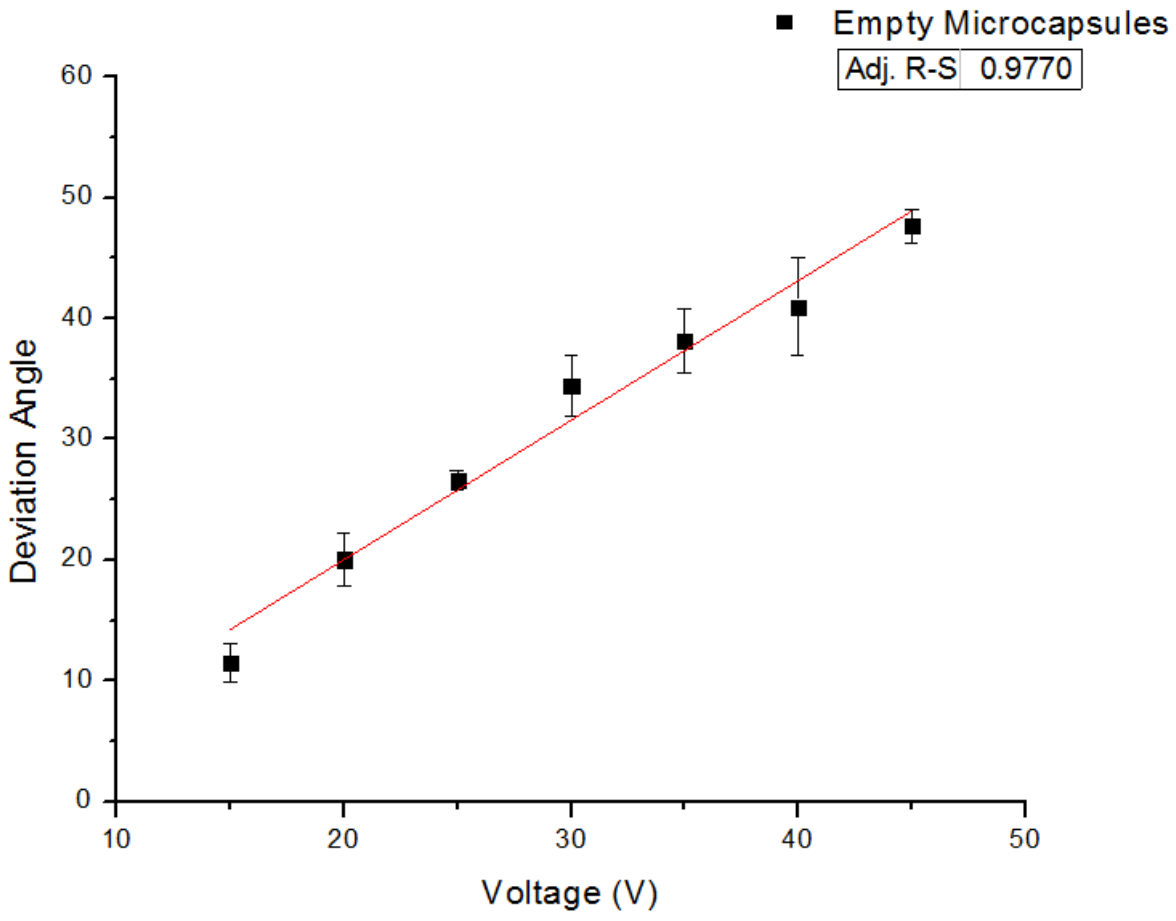

Figure 26. Deviation angle of empty microcapsules vs voltage applied at 15-45V. Error bars represent the standard deviation of deviation angle with n=3 i.e. 3 microcapsules tested at each voltage.

Trends shown by the microcapsules under the DC electric field demonstrate a linear relationship between the voltage applied and the deviation angle recorded. The experiment was repeated on at least 3 different devices with different set of empty microcapsules prepared fresh each time. It was observed that with an increase in the applied voltage, the deviation angle also increased. It can be concluded that the deviation of microcapsules is easily tunable with the electric field applied. At the same time, flow rate of the fluid medium of the microcapsules within the DLD-EP device can have a substantial effect on the deviation angle. Due to this, in order to maintain a certain deviation angle, the electric field would need to be adjusted according to the flow rate. Therefore, in the next section, we try to compare the deviation angle of a different sample set containing polystyrene beads-laden microcapsules and empty ones.

4.6 Results and Discussion

4.6.1 Characterization of Empty vs Polystyrene Beads Microcapsules in DLD-EP

The goal for introducing empty and polystyrene beads-laden microcapsules into the DLD-EP device was to observe a significant difference between their deviation angles in response to an electric field. From *Chapter 3,* we know that polystyrene beads-laden microcapsules in response to electric field travel at a slower speed in comparison to the empty ones. Therefore, the hypothesis is that, their deviation angle under the combined effect of DLD and EP should be lower in comparison to empty microcapsules. To access this hypothesis, both samples were introduced into the microfluidic channel at a constant flow rate, slow enough to examine the microcapsule behavior under DLD-EP conditions. A voltage difference, ranging from 15 to 45V, was applied across the channel width and the response was analyzed (at least three microcapsules per experimental condition). The results are summarized in *Figure 27*.

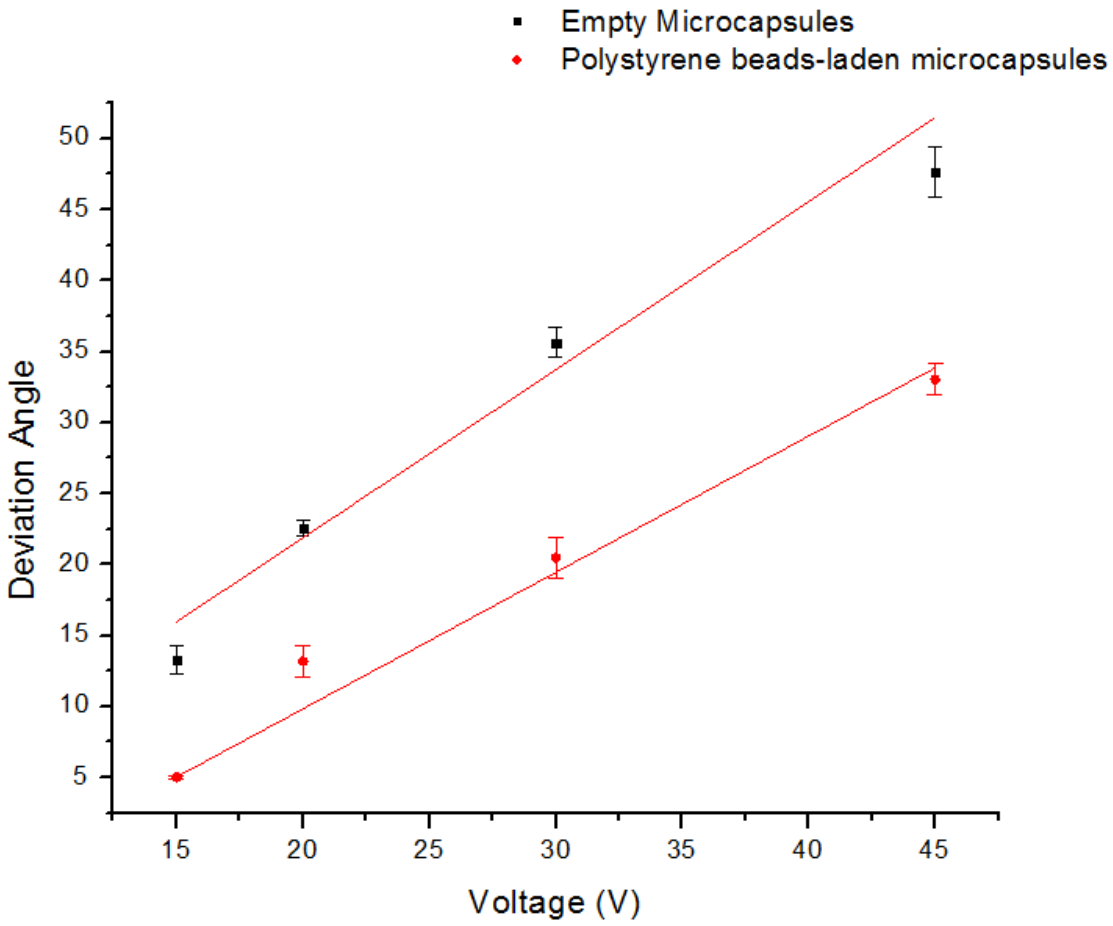

Figure 27. Deviation angle of empty & polystyrene beads-laden microcapsules vs voltage applied, Error bars represent the standard deviation of deviation angle with n=3, all microcapsules sized between 55-60µm. R^2 value for empty microcapsule – 0.93 and beads-laden microcapsule – 0.98

Two trends were observed, wherein the deviation angle was seen to increase with the applied voltage. The experiment was repeated on at least 3 different devices with new set of microcapsules freshly prepared. A notable observation was that empty microcapsules were seen to deviate more than the microcapsules with polystyrene-beads in them. These experimental findings agree with our initial hypothesis that the beads-laden microcapsules would deviate less than the empty ones. This data also correspond to results obtained in *Chapter 2* that the empty microcapsules travel at a faster terminal velocity than the beads-laden microcapsules. With these promising results, the next steps would be to continue testing on DLD-EP device using cell laden microcapsules.

4.6.2 Characterization of Empty vs Cell-laden Microcapsules in DLD-EP

The goal of introducing cell-laden microcapsules into the DLD-EP device was to formulate a trend as seen with polystyrene beads-laden microcapsules in *Figure 27*. Comparing the data in *Section 2.6.1 EP for Empty microcapsules vs Cell-laden microcapsules*, we know that cell-laden microcapsules carry a higher net negative charge since they travel at a higher velocity than empty ones.

Using cells for experimentation has always been a challenge and the same was noticed while performing experiments under DLD-EP. The encapsulation process involves using SPAN-80 which is a non-ionic reagent that reduces surface tension between multiple microcapsules, preventing coalescence. Even with this precaution, clumping of cell-laden microcapsules, post encapsulation was one such challenge observed, which eventually led to clogging of the DLD-EP device. Mitigations involved lowering centrifuge speeds and increasing number of cycles during the oil removal step after encapsulation. Another crucial challenge was the 'Sticking' issue- microcapsules getting stuck in and around the microfluidic channel and pillars as shown in *Figure 28*. This is primarily due to the adhesive nature of cells and agarose [64]. Several strategies were applied to mitigate the stickiness issue which is summarized in *Table 3*.

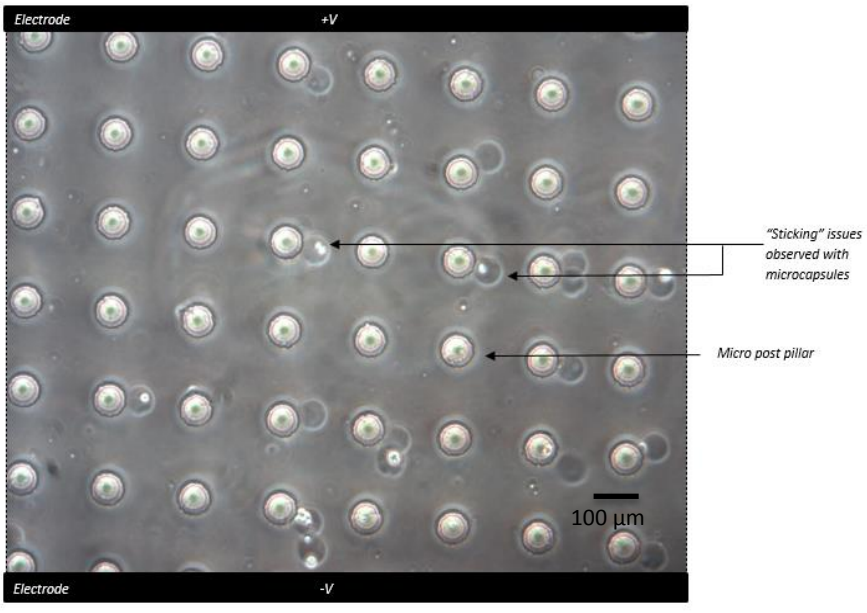

Figure 28. Cell-laden microcapsules 'sticking' issues depicted in a section of DLD-EP device.

Strategy	Workflow	Efficiency
Adding Bovine Serum Albumin (BSA) 0.1 mg/mL	Unspecific binding of microcapsules can be avoided by coating BSA on the microfluidic surface, as BSA forms a protein layer over the PDMS surface [65].	Even though BSA significantly reduced sticking, it led to a new problem- inconsistent electric field, which could be due to its negative nature [66]. Therefore, BSA was not used.
Plasma Treatment	Plasma treatment is used to alter the surface chemistry of a microfluidic channel to hydrophilic [67]. Two different combinations of plasma treatment were tested: ● *0.3 minutes - 30Watts* ● *5 minutes - 50Watts*	● *0.3 minutes, 30W* - No sticking observed in upto 5 minutes of microcapsules entry, however sticking began >5 minute, which may be due to loss of plasma integrity ● *5 minutes, 50W* - Caused melting of electrode and ultimately led to device damage Plasma for 0.3 minutes, 30W with improvements, can be used for further experimentation.
KCl- Glycerol	KCl has been used extensively as conductive media for electrophoresis experiments [68] For our experiments KCl-Glycerol substituted LCM, while maintaining low-conductivity for higher cell viability. However, a small amount of salt is necessary for electrophoresis to work. 0.092g or 70µL of Glycerol was dissolved in 3.33 mL of 100uM KCl. This ratio was considered to maintain the osmolarity between the solution and cells (260-300 mOsmol/L) [69] to promote homeostasis and promote cell viability.	KCl-Glycerol yielded better results in terms of the sticky issue, compared to LCM. There was no erratic behavior of microcapsules under an applied electric field, they continued to deviate from their original pathway as expected.

PEG-Silane	PEG-Silane is generally used to avoid non-specific binding and prevent surface modifications of microfluidic channels [70]. In our study, 3mM PEG-Silane (SIM 6492.7) was dissolved in 44mL of 10mM HCl (Protocol adapted from tabard-cossa lab member). Prior to coating with PEG-Silane, plasma treatment of 0.3 minutes and 30W was performed. Incubation period of ~20-30 minutes was given for coating. PEG-Silane was flushed out of the microfluidic device by flowing H_2O across the channel. This method was adopted and modified from *Hellmich, et al., 2005.*	PEG-Silane overall showed by far, the best improvements in preventing the sticky behavior of microcapsules, therefore it was used for all future experiments. However, there is still room for improvement.

Table 3 Strategies used to overcome microcapsule flow challenges within the DLD-EP microfluidic channel.

Our experiments showed that KCl-Glycerol and PEG-Silane treatment, when used in combination, yielded the best results in terms of microcapsule stickiness mitigation. Subsequently, all microcapsules (cell-laden and empty) used for DLD-EP experimentation were collected in a KCl-Glycerol solution. PEG-Silane treatment was performed in combination with the plasma treatment as discussed earlier in this section. The results are summarized in *Figure 30.*

Viability under DLD-EP conditions: Cells under DC electric field conditions have shown promising viability [73]. However, viability is often decreased with an increase in time. Therefore, for our experiments, we may assume that cells do not lose their viability over the short period of time from encapsulation to DLD-EP experimentation. To test this hypothesis, a small review on cell viability assay using Trypan Blue 0.4% W/V was performed. Cell-laden microcapsules were incubated with Trypan Blue for ~4-5 minutes to allow infusion of dye into the cells. Then, 10 µl of the sample was dropped onto a hemocytometer and visualized under a microscope. For our experiment, cell-laden microcapsules were examined both before and after the DLD-EP experiment. Dye was taken up by the dead cells and looked dark, whereas, live cells looked bright. Results showed that there was no sudden drop in viability as shown by *Figure 29*. For future work, quantifying the viability assay by counting the number of cell-laden (live) microcapsules by comparing with the outlet (dead) may give a better outlook.

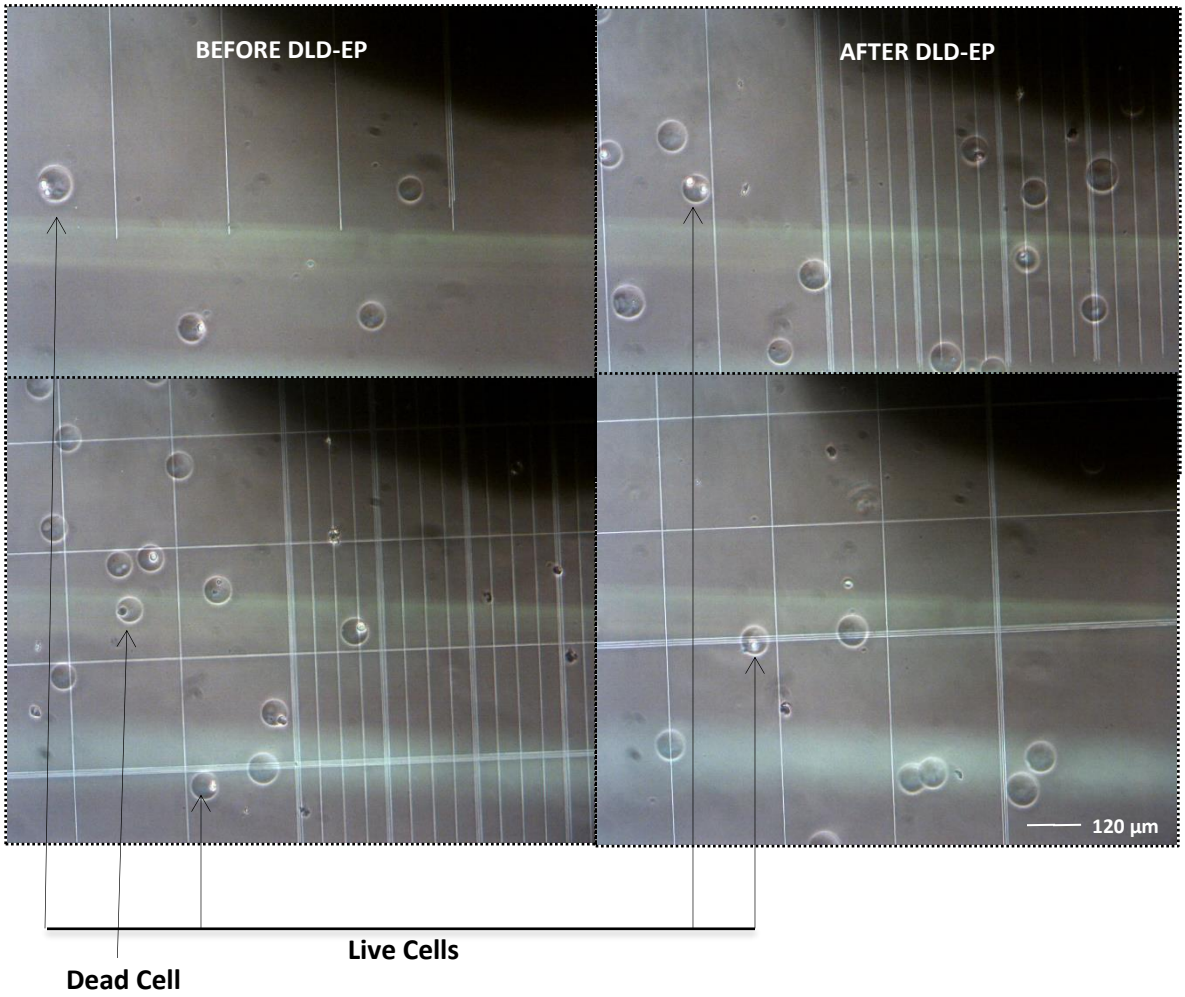

Figure 29. Cell-viability assay performed by using Trypan Blue (0.4% W/V) staining of cells. Dead cells take up the dye and appear dark whereas live cells appear bright. Both before and after experiment (DLD-EP) images of cell-laden microcapsules show positive viability.

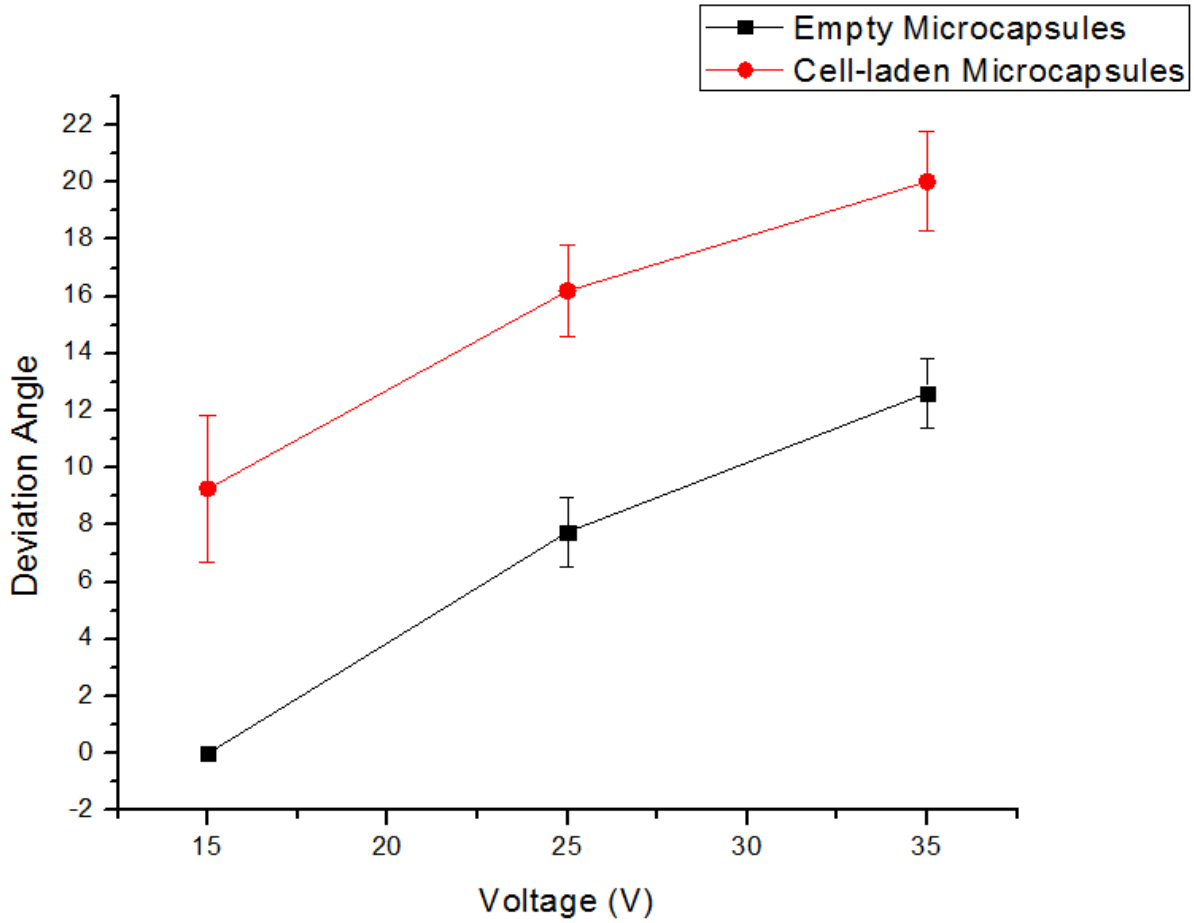

Figure 30. Deviation angle of empty microcapsules & cell-laden vs voltage applied, all microcapsules sized between 55-60µm and suspended in a KCl-Glycerol solution 118.5 µL/min flow rate.

With all these corrective measures in place, the experimental results are summarized in *Figure 30* which shows the trends between the voltage applied and the deviation angle observed at a constant flow rate. Cell-laden and empty microcapsules at once enter through the $Inlet_1$, keeping the flow rate constant (for visualization under microscope). A section of DLD was then used for recording data for DLD-EP through similar fashion explained under *Section 4.4 Quantification*. The data observed under DLD-EP corresponds with the results seen in *Chapter 2* where cell-laden microcapsules travelled faster (with a higher net negative charge) than empty microcapsules. Therefore, by that theory they should deviate higher than empty ones, which is what we notice in *Figure 30* as well. In the future, if a better strategy can be adopted to improve the sticking issues of microcapsules, a higher precision in the above data set may be achieved.

4.7 Deviation Angle as a Sorting Factor

It was experimentally concluded that a significant difference was seen between two sets of microcapsules (‘*empty vs cell-laden’* and ‘*empty vs polystyrene beads-laden’*) tested under the influence of DLD-EP.

Therefore, we can conclude that the deviation angle can be used as a successful sorting factor for cell-laden and empty microcapsules. In the future, experimentation can be performed to quantify sorting behavior. This can be done by comparing the ratio of microcapsule mixture sample at the inlet and counting the sorted microcapsules at two outlets respectively.

CHAPTER 5

5.1 Conclusion

Cell encapsulation has shown potential in eliminating the challenges experienced during administration of stem cells directly into the patient. Encapsulating stem cells within the hydrogel material aids in preventing loss of cell retention rate, and cell viability against the host immune system ultimately improving their therapeutic effect. Through droplet-based microfluidics, encapsulating stem cells into uniform microspheres has become relatively accessible. It offers the opportunity to manually regulate the size of the microcapsules via pressure-controlled regulators while maintaining high throughput. However, due to the random nature (Poisson distribution), there are often cases where microcapsules produced do not contain any cells in them. Thus, a significant amount of empty hydrogel microcapsules with no remedial influence is introduced into the subject. Hence, there is a need to sort cell-laden microcapsules from the empty ones. Considerable number of approaches have been made towards separating the two sets of microcapsules, most of them focused on the means of active sorting *i.e.* by utilizing and/or altering the characteristics of stem cells. Deterministic Lateral Displacement (DLD) - Electrophoresis (EP) presents a label-free, non-invasive sorting platform to effectively distinguish between empty and occupied microcapsules. Each technique offers its own asset, and the goal of our study presented a system to integrate both into a single platform. The two means were first examined individually to understand and identify the difference in behavior of empty and occupied microcapsules.

EP means alone was practiced to characterize microcapsules based on their net charge. Motion of empty and occupied microcapsules inside a microfluidic platform was captured and translated into velocity measured against different electric fields. Trends from EP experiments distinctly demonstrated that there is a significant difference in the terminal velocity for empty and occupied microcapsules i.e., there is a difference in their net negative charge. It was shown that cell-laden microcapsules at three different electric fields of 50V/cm, 150V/cm and 200V/cm travelled at a faster rate (~twice) compared to empty microcapsules. Polystyrene beads (~11 µm) were used as a substitute for cell-laden microcapsules as it offers a considerable advantage

of fastening the encapsulation process being easy to handle and work with. Interestingly, polystyrene beads-laden microcapsules velocity under the influence of electric field was slower compared to empty microcapsules. Certain irregularities in the actual numbers in the velocity were observed in the two sets of experiments. This was recognized as an effect of presence & absence of salt as well as changes in the agarose concentrations and poor filtration of the cell culture media. However, for a given experiment, the conditions were stable enough to uncover different mobility and the two linear trends never tend to intersect each other. Another detail noticed was the fact that all sets of microcapsules- empty, cell-laden and polystyrene beads-laden were negatively charged. Therefore, applying EP alone in a microfluidic setup would not have been enough to allow sorting of our sample effectively.

DLD is a hydrodynamic approach that is used for sorting of a sample based primarily on their difference in size. In our study, imposing DLD and EP together were employed towards building a platform for separating empty and occupied microcapsules. By introducing micro-posts obstacles or pillars in front of the microcapsules, we intended on creating a much wider difference between the two models. DLD array tends to deflect all microcapsules into a selective pathway, whereas the electric field induced due to the lateral electrodes deviate occupied microcapsules into a different trajectory. During our characterization using the DLD-EP study, we were able to demonstrate a difference between the deviation angles for the three sets of microcapsules- empty, cell-laden and polystyrene beads-laden. It was noted that polystyrene beads-laden microcapsules deviated less compared to empty ones corresponding to their EP trends. Using cell-laden microcapsules under DLD-EP conditions seemed challenging at first. Comparable strategies were then applied towards the challenges of ‘Clumping’ and ‘Sticking’, which resulted in replacing our suspension media from LCM (8.5% Sucrose & 0.3% Dextrose) to KCl-Glycerol, followed by coating the microfluidic channels with PEG-Silane. With improvements witnessed after applying these strategies, DLD-EP experiments were resumed and the trends for cell-laden microcapsule deviating more than empty microcapsules was observed while maintaining a constant flow rate. In order to extend the possible shortcomings of the DLD-EP strategy, few means of leveraging ‘deviation angle’ towards sorting of occupied and empty microcapsules was described.

To conclude, in our thesis, an exciting prospect on the study of sorting cell-laden microcapsules was put forward. We were able to design and fabricate a microfluidic platform composed of a DLD array sandwiched between two lateral electrodes. Our initial experiments involved investigating the behavior of empty and occupied (cell-laden & polystyrene beads-laden) microcapsules under the influence of electric field alone. Difference in their velocities signified the need of DLD for sorting. Introducing electric field into the action deviates occupied microcapsules (cell-laden) towards a different trajectory, as opposed to empty microcapsules which deviate as well but significantly lower due to the presence of micro-post pillars. Few upgrades on the size of the microfluidic platform can be adjusted to facilitate the sorting, other improvements that can benefit towards high occupancy and efficiency of the encapsulation are looked into under the next section.

5.2 Future work

As we know that all microcapsules carry a net negative charge, changing the charge of empty or occupied microcapsules can potentially serve as an intriguing approach towards creating a broad variation between the two models. Adjusting the charge of cells seems to be an accessible scheme and some foundation work was done as shown through *Figure. 31*. This involved coating 3T3 cells within a single mono layer of Poly-L-Lysine [71][72] and studying the behavior of only cells under our EP microfluidic settings. The change of charge seen in the cells from negative to positive, demonstrated promising results. However, challenges appeared after encapsulating these poly-l-lysine coated cells. The microcapsules failed to show any change in their net charge which could be due to the release/loss of the poly-l-lysine coating over the encapsulation period. Therefore, an improved protocol could potentially be applied in order to change the net charge of occupied microcapsules to positive allowing us to easily sort them based on the methods presented in this thesis.

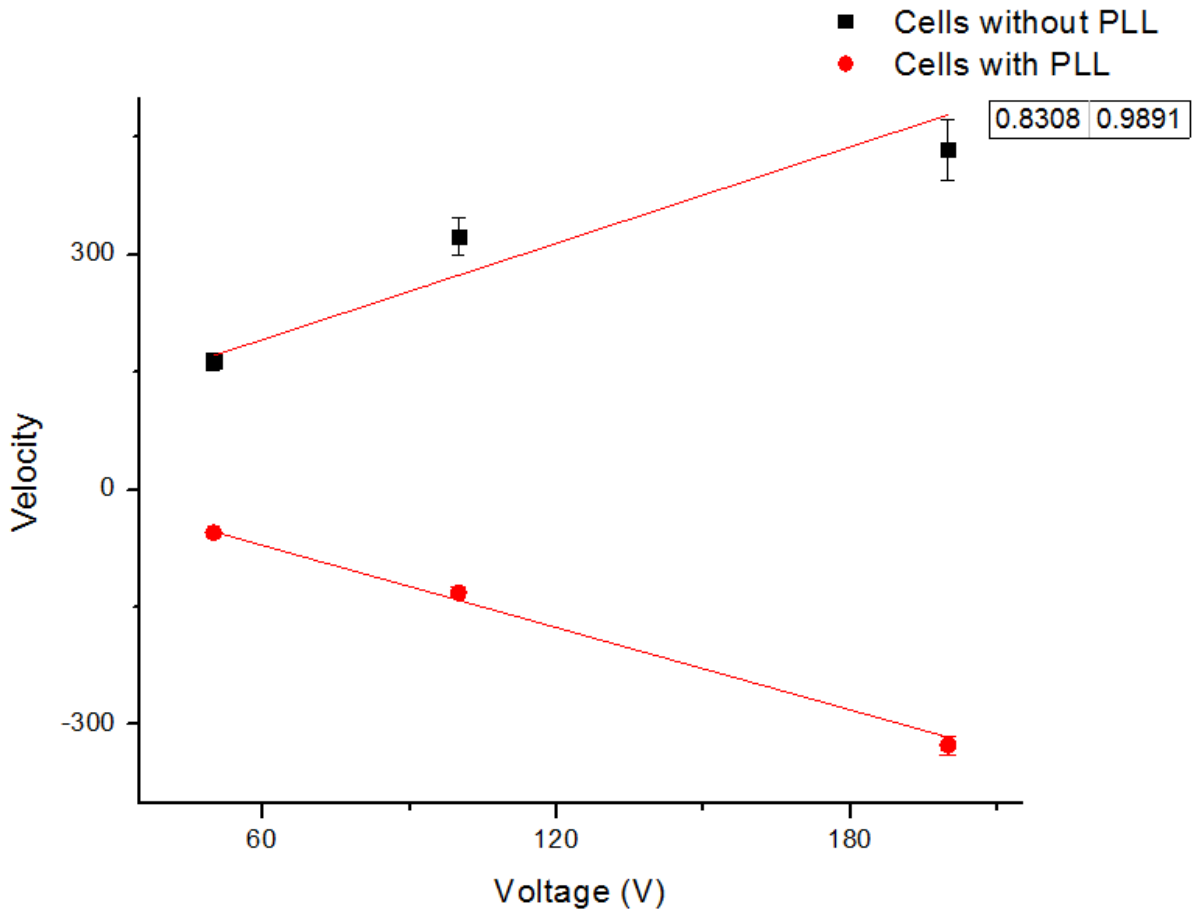

Figure 31. Graph for Cells (3T3) coated with poly-L-lysine and without coating demonstrating change in the charge of cell from negative to positive (n=3).

Another side of the microfluidics approach which is yet to be explored is the integration of the sorting strategy with the encapsulation setup itself. Such a complex setup however, would offer a vast improvement over other techniques currently out there. The microcapsules generated can be directed into the DLD-EP device eliminating all intermediary steps, overall automating the entire process and reducing the time. In order to accomplish this, mineral oil (in which microcapsules are collected) would need to be replaced with a conductive oil, so integration of DLD-EP and encapsulation setup is possible. Occupied microcapsules collected in a specific outlet can later be separated from oil via centrifugation.

Using the lateral electrodes before droplet generation could prove to be a promising strategy as well. The electric field will deviate the aqueous mixture of cells and agarose into a different channel, releasing a much more concentrated solution of cells into the encapsulation region. This technique however, disrupts the regulation of producing microcapsules with fewer number of cells per capsule.

Changing the pH of the collection media may have a positive effect in changing the net charge of agarose/cells. This brings into play, the concept of isoelectric focusing. It involves adjusting the charge of the particle by changing the pH of the medium it is collected in. For instance, collecting microcapsules in an acidic or basic medium may create a difference in the charge of agarose relative to the cell. Numerous strategies were adopted to deal with the challenges of using cell-laden microcapsules in DLD-EP experiments. Changing the collection media for microcapsules seemed to show a positive effect in solving those issues. In the future, choosing a better protocol for coating the microfluidic channels over the ones presented in this study could show a favorable outcome in compiling significant statistics.

References

[1] Li, X., Tamama, K., Xie, X., & Guan, J. "Improving Cell Engraftment in Cardiac Stem Cell Therapy" Stem cells international, 2016, 7168797. doi:10.1155/2016/7168797

[2] Fong, E. J., Huang, C., Hamilton, J., Benett, W. J., Bora, M., Burklund, A., … Shusteff, M " A Microfluidic Platform for Precision Small-volume Sample Processing and Its Use to Size Separate Biological Particles with an Acoustic Microdevice" Journal of visualized experiments : JoVE, (105), 53051. doi:10.3791/53051, 2015

[3] Au, A. K., Bhattacharjee, N., Horowitz, L. F., Chang, T. C., & Folch, A "3D-printed microfluidic automation". Lab on a chip, 15(8), 1934–1941. doi:10.1039/c5lc00126a, 2015

[4] Stefan Haeberlea and Roland Zengerleab "Microfluidic platforms for lab-on-a-chip applications" Lab on a chip, DOI: 10.1039/b706364b, 2007

[5] J. Kirby "Micro- and Nanoscale Fluid Mechanics Transport in Microfluidic Devices", Cornell University, New York, isbn: 9780521119030, 2010

[6] Wei-Lung Chou, Pee-Yew Lee, Cing-Long Yang, Wen-Ying Huang and Yung-Sheng Lin "Recent Advances in Applications of Droplet Microfluidics", Micromachines, 2015

[7] Marco Zaky Elizabeth Swanson and Jay Mistri "Laminar Flow", Retrieved from openwetware.org (17 February 2017)

[8] Andreas H. Kunding, Louise L. Busk, Helen Webb, Hans W. Klafki, Markus Otto, Jörg P. Kutter and Martin Dufva "Micro-droplet arrays for micro-compartmentalization using an air/water interface" Lab on a chip, DOI: 10.1039/c8lc00608c, 2017

[9] Nachiket Shembekar, Chawaree Chaipan, Ramesh Utharala and Christoph A. Merten "Droplet-based microfluidics in drug discovery, transcriptomics and high-throughput molecular genetics", Lab on a chip,DOI: 10.1039/c6lc00249h, 2016

[10] Pagaduan, J. V., Sahore, V., & Woolley, A. T. "Applications of microfluidics and microchip electrophoresis for potential clinical biomarker analysis" Analytical and bioanalytical chemistry, 407(23), 6911–6922. doi:10.1007/s00216-015-8622-5, 2015

[11] Lina Wu, "Droplet Microfluidics: T-Junction", Retrieved from openwetware.org

[12] Pingan Zhuab and Liqiu Wang "Passive and active droplet generation with microfluidics: a review", Lab on a chip, DOI: 10.1039/c6lc01018k, 2017

[13] Charles N. Baroud, Francois Gallaireb and Remi Dangla "Dynamics of microfluidic droplets", RSC, DOI: 10.1039/c001191f, 2010

[14] Ali Lashkaripour, Christopher Rodriguez,Luis Ortiz ad and Douglas Densmore "Performance tuning of microfluidic flow-focusing droplet generators", Lab on a chip, DOI: 10.1039/c8lc01253a, 2019

[15] XiaomingChen and Carolyn L.Ren "Experimental study on droplet generation in flow focusing devices considering a stratified flow with viscosity contrast", Chemical Engineering Science Volume 163, https://doi.org/10.1016/j.ces.2017.01.029, 2017

[16]Venoos Amiri Roodan "Computational Analysis of Magnetic Droplet Generation and Manipulation in Microfluidic Devices", University at Buffalo, State University of New York, 2018

[17] Zhao, S., Xu, Z., Wang, H., Reese, B. E., Gushchina, L. V., Jiang, M., … He, X. "Bioengineering of injectable encapsulated aggregates of pluripotent stem cells for therapy of myocardial infarction". Nature communications, 7, 13306. doi:10.1038/ncomms13306, 2016

[18] Matthias Stelljes, Robert Strothotte, Hans-Gerd Pauels, Christopher Poremba, Michaela Milse, Christiane Specht, Jörn Albring, Guido Bisping, Christian Scheffold, Thomas Kammertoens, Elisabeth Oelmann, Gerda Silling, Wolfgang E. Berdel, Joachim Kienast "Graft-versus-host disease after allogeneic hematopoietic stem cell transplantation induces a CD8+ T cell-mediated graft-versus-tumor effect that is independent of the recognition of alloantigenic tumor targets",Blood, 104 (4) 1210-1216; DOI: 10.1182/blood-2003-10-3387, 2004

[19] McLeod, C. J., Wang, L., Wong, C., & Jones, D. L. "Stem cell dynamics in response to nutrient availability",Current biology : CB, 20(23), 2100–2105. doi:10.1016/j.cub.2010.10.038, 2010

[20] Yvette Brazier "What are stem cells, and what do they do?", Retrieved from https://www.medicalnewstoday.com, 2018

[21] Zhang, Q., & Austin, R. H. "Applications of Microfluidics in Stem Cell Biology", BioNanoScience, 2(4), 277–286. doi:10.1007/s12668-012-0051-8, 2012

[22] Ludwinski, F. E., Patel, A. S., Damodaran, G., Cho, J., Furmston, J., Xu, Q., Modarai, B. "Encapsulation of macrophages enhances their retention and angiogenic potential". NPJ Regenerative medicine, 4, 6. doi:10.1038/s41536-019-0068-5, 2019

[23] Woojin M. Han, Shannon E. Anderson, Mahir Mohiuddin, Daniela Barros, Shadi A. Nakhai, Eunjung Shin, Isabel Freitas Amaral, Ana Paula Pêgo, Andrés J. García and Young C. Jang "Synthetic matrix enhances transplanted satellite cell engraftment in dystrophic and aged skeletal muscle with comorbid trauma", Science Advances, 2018

[24] Hsiu-Wen Chien, Xuewei Xu, Jean-Rene Ella-Menye, Wei-Bor Tsai, and Shaoyi Jiang Langmuir "High Viability of Cells Encapsulated in Degradable Poly(carboxybetaine) Hydrogels", Langmiur, 28 (51), 17778-17784 DOI: 10.1021/la303390j, 2012

[25] Geckil, H., Xu, F., Zhang, X., Moon, S., & Demirci, U "Engineering hydrogels as extracellular matrix mimics" Nanomedicine (London, England), 5(3), 469–484. doi:10.2217/nnm.10.12, 2010

[26] Rana Imani, Shahriar Hojjati Emami, Parisa Rahnama Moshtagh, Nafiseh Baheiraei & Ali Mohammad Sharifi "Preparation and Characterization of Agarose-Gelatin Blend Hydrogels as a Cell Encapsulation Matrix: An In-Vitro Study", Journal of Macromolecular Science, Part B, 51:8, 1606-1616, DOI: 10.1080/00222348.2012.657110, 2012

[27] Broche, L. M., Hoettges, K. F., Ogin, S. L., Kass, G. E. and Hughes, M. P. "Rapid, automated measurement of dielectrophoretic forces using DEP-activated microwells" ELECTROPHORESIS, 32: 2393-2399. doi:10.1002/elps.201100063, 2011

[28] Annabi, N., Nichol, J. W., Zhong, X., Ji, C., Koshy, S., Khademhosseini, A., & Dehghani, F. "Controlling the porosity and microarchitecture of hydrogels for tissue engineering" Tissue engineering. Part B, Reviews, 16(4), 371–383. doi:10.1089/ten.TEB.2009.0639,2010

[29] Z. Jiang, B. Xia, R. McBride, and J. Oakey "A microfluidic-based cell encapsulation platform to achieve high long-term cell viability in photopolymerized PEG hydrogel microspheres", J. Mater. Chem. B Mater. Biol. Med., vol. 5, no. 1, pp. 173–180, 2017

[30] Benavente-Babace, A, Haase, K, Stewart, DJ, Godin, M. "Strategies for controlling egress of therapeutic cells from hydrogel microcapsules" J Tissue Eng Regen Med; 13: 612– 624. https://doi.org/10.1002/term.2818, 2019

[31] "Cell culture guidelines", abcam ®discover more retrieved from www.abcam.com

[32]Monette Catafard Nicolas "High throughput cell encapsulation in monodisperse agarose microcapsules using a microfluidic device", University of Ottawa, Canada, 2014

[33] SU-8 2000 "Permanent epoxy negative photoresist processing guidelines SU-8 2025, SU-8 2035, SU-8 2050 and SU-8 2075", Micro Chem ®retrieved from www.microchem.com

[34] Calixto Saenz "Procedure for silanization of SU-8/Silicon Master", Microfabrication Core Facility, Harvard Medical School retrieved from hms.harvard.edu, 2015

[35] Dr. Alex Iles, "Plasma Treatment of PDMS for Microfluidic", Henniker Plasma, retrieved from plasmatreatment.co.uk

[36] Rushi Panchal, "Tracking egress of doubly encapsulated cells", University of Ottawa, Canada, (2019)
[37] David J. Collins, Adrian Neild, Andrew deMello, Ai-Qun Liud and Ye Ai "The Poisson distribution and beyond: methods for microfluidic droplet production and single cell encapsulation", Lab on a Chip, DOI: 10.1039/c5lc00614g, 2015

[38] Jeremy J. Agresti, Eugene Antipov, Adam R. Abate, Keunho Ahn, Amy C. Rowat, Jean-Christophe Baret, Manuel Marquez, Alexander M. Klibanov, Andrew D. Griffiths, David A. Weitz "Ultrahigh-throughput screening in drop-based microfluidics for directed evolution" ,Proceedings of the National Academy of Sciences, 107 (9) 4004-4009; DOI: 10.1073/pnas.0910781107, 2010

[39] Nam, J., Lim, H., Kim, C., Yoon Kang, J., & Shin, S. "Density-dependent separation of encapsulated cells in a microfluidic channel by using a standing surface acoustic wave". Biomicrofluidics, 6(2), 24120–2412010. doi:10.1063/1.4718719, 2010

[40] Tengyang Jing, Ramesh Ramji, Majid Ebrahimi Warkiani, Jongyoon Han, Chwee Teck Lim, Chia-Hung Chen "Jetting microfluidics with size-sorting capability for single-cell protease detection", Biosensors and Bioelectronics, Volume 66, 2015,ISSN 0956-5663,https://doi.org/10.1016/j.bios.2014.11.001, 2014

[41] Gutzweiler, Gleichmann, Tanguy, Koltay, Zengerle, Riegger "Open microfluidic gel electrophoresis: Rapid and low cost separation and analysis of DNA at the nanoliter scale", Electrophoresis,doi: 10.1002/elps.201700001, 2017

[42] Wang G, Mao W, Byler R, Patel K, Henegar C, et al "Stiffness Dependent Separation of Cells in a Microfluidic Device" PLOS ONE 8(10): e75901. https://doi.org/10.1371/journal.pone.0075901, 2013

[43] Yuke Li, Hongna Zhang, Yongyao Li, Xiaobin Li, Jian Wu, Shizhi Qian & Fengchen Li "Dynamic control of particle separation in deterministic lateral displacement separator with viscoelastic fluids", Scientific Reports,volume 8, Article number: 3618, 2018

[44] John Alan Davis "Microfluidic Separation of Blood Components through Deterministic Lateral Displacement", Princeton University, 2008

[45] Pagaduan, J. V., Sahore, V., & Woolley, A. T. "Applications of microfluidics and microchip electrophoresis for potential clinical biomarker analysis" Analytical and bioanalytical chemistry, 407(23), 6911–6922. doi:10.1007/s00216-015-8622-5, 2015

[46] B. J. Kirby "Micro-and Nanoscale Fluid Mechanics -Transport in Microfluidic Devices", Cambridge: Cambridge University Press, 2010

[47] Broche, L. M., Hoettges, K. F., Ogin, S. L., Kass, G. E. and Hughes, M. P. "Rapid, automated measurement of dielectrophoretic forces using DEP-activated microwells". ELECTROPHORESIS, 32: 2393-2399. doi:10.1002/elps.201100063, 2011

[48] D. W. Renn "Agar and agarose: Indispensable partners in biotechnology", Industrial & Engineering Chemistry Product Research and Development, 1984

[49] RMP Laboratory, "RMP > Theory", The McGill Physiology Virtual Lab retrieved from www.medicine.mcgill.ca

[50] Meenakshi Arora, "Cell Culture Media: A Review", Labome, //dx.doi.org/10.13070/mm.en.3.175, 2013

[51] Puttaswamy, S. V., Sivashankar, S. , Chen, R. , Chin, C. , Chang, H. and Liu, C. H. "Enhanced cell viability and cell adhesion using low conductivity medium for negative dielectrophoretic cell patterning". Biotechnology Journal, 5: 1005-1015. doi:10.1002/biot.201000194, 2010

[52] Im, D. J., Noh, J., Yi, N. W., Park, J., & Kang, I. S. "Influences of electric field on living cells in a charged water-in-oil droplet under electrophoretic actuation". Biomicrofluidics, 5(4), 44112–4411210. doi:10.1063/1.3665222, 2011

[53] M Stacey, J Stickley, P Fox, V Statler, K Schoenbach, S.J Beebe, S Buescher "Differential effects in cells exposed to ultra-short, high intensity electric fields: cell survival, DNA damage, and cell cycle analysis,'' Mutation Research/Genetic Toxicology and Environmental Mutagenesis, Volume 542, Issues 1–2, Pages 65-75, ISSN 1383-5718, https://doi.org/10.1016/j.mrgentox.2003.08.006, 2003

[54] Cooper, "Structure of the Plasma Membrane", The Cell: a molecular approach, 2nd Edition, 2000

[55] Ma, Y., Poole, K., Goyette, J., & Gaus, K. "Introducing Membrane Charge and Membrane Potential to T Cell Signaling" Frontiers in immunology, 8, 1513. doi:10.3389/fimmu.2017.01513, 2017

[56] M. Pekker, M.N. Shneider, "The surface charge of a cell lipid membrane" J Phys Chem Biophys, DOI: 10.4172/2161-0398.1000177, 2015

[57] "Polymer Microspheres, Tech Note 100", Bangs Laboratories Inc, retrieved from www.bangslabs.com

[58] Fondriest Staff, "What is Conductivity?", Environmental Monitor, 2010

[59] Eloise Pariset, Jean Berthier, Catherine Pudda, Fabrice Navarro, Béatrice Icard and Vincent Agache, "Particle Separation with Deterministic Lateral Displacement (DLD): The Anisotropy Effect", Proceedings, Eurosensors Paris, 2017

[60] Naotomo Tottori, Takasi Nisisako, Jongho Park, Yasuko Yanagida, and Takeshi Hatsuzawa, "Separation of viable and nonviable mammalian cells using a deterministic lateral displacement microfluidic device", Biomicrofluidics, https://doi.org/10.1063/1.4942948, 2016

[61] Holmes David, Whyte Graeme, Bailey Joe,Vergara-Irigaray Nuria, Ekpenyong Andrew, Guck Jochen and Duke Tom "Separation of blood cells with differing deformability using deterministic lateral displacement", Interface Focus http://doi.org/10.1098/rsfs.2014.0011, 2014

[62] Zeming, Kerwin Kwek et al. "Asymmetrical Deterministic Lateral Displacement Gaps for Dual Functions of Enhanced Separation and Throughput of Red Blood Cells." Scientific reports vol. 6 22934. 10, doi:10.1038/srep22934, 2016

[63] "HOW TO SUCCEED YOUR SU-8 PHOTORESIST UV EXPOSURE?", Elveflow, retrieved from www.elveflow.com

[64] Yoshihide Furuichi, Keita Iwasaki & Katsutoshi Hori, "Cell behavior of the highly sticky bacterium Acinetobacter sp. Tol 5 during adhesion in laminar flows", Nature, DOI:10.1038/s41598-018-26699-5, 2018

[65] Schrott, W., Slouka, Z., Cervenka, P., Ston, J., Nebyla, M., Pribyl, M., & Snita, D. "Study on surface properties of PDMS microfluidic chips treated with albumin" Biomicrofluidics, 3(4), 44101. doi:10.1063/1.3243913, 2009

[66] Phan, H. T., Bartelt-Hunt, S., Rodenhausen, K. B., Schubert, M., & Bartz, J. C. "Investigation of Bovine Serum Albumin (BSA) Attachment onto Self-Assembled Monolayers (SAMs) Using Combinatorial Quartz Crystal Microbalance with Dissipation (QCM-D) and Spectroscopic Ellipsometry (SE)" PloS one, 10(10), e0141282. doi:10.1371/journal.pone.0141282, 2015

[67] https://www.thierry-corp.com/plasma/knowledge/hydrophilic-treatment/

[68] Hellman, L. M., & Fried, M. G. "Electrophoretic mobility shift assay (EMSA) for detecting protein-nucleic acid interactions" Nature protocols, 2(8), 1849–1861. doi:10.1038/nprot.2007.249, 2007

[69] Predrag Vujovic, Michael Chirillo, and Dee U. Silverthorn, "Learning (by) osmosis: an approach to teaching osmolarity and tonicity", Advances in Physiology Education, https://doi.org/10.1152/advan.00094, 2018

[70] Kyle M. Kovach, Jeffrey R. Capadona, Anirban Sen Gupta, Joseph A. Potka, "The effects of PEG-based surface modification of PDMS microchannels on long-term hemocompatibility", J Biomed Mater Res A, doi: 10.1002/jbm.a.35090, 2014

[71] C. Picart, Ph. Lavalle, P. Hubert, F. J. G. Cuisinier, G. Decher, P. Schaaf and J.-C. Voegel, "Buildup Mechanism for Poly (L-lysine)/Hyaluronic Acid Films onto a Solid Surface", Langmuir 17237414-7424, 2001

[72] Heo, J. S., Kim, H. O., Song, S. Y., Lew, D. H., Choi, Y., & Kim, S. " Poly-L-lysine Prevents Senescence and Augments Growth in Culturing Mesenchymal Stem Cells Ex Vivo" BioMed research international, 8196078. doi:10.1155/2016/8196078, 2016

[73] Min Zhao, Andrew Dick, John V. Forrester, and Colin D. McCaig, "Electric Field–directed Cell Motility Involves Up-regulated Expression and Asymmetric Redistribution of the Epidermal Growth Factor Receptors and Is Enhanced by Fibronectin and Laminin", Molecular Biology of the CellVol. 10, No. 4, https://doi.org/10.1091/mbc.10.4.1259, 2017